Regulation of the poly(A) status of mitochondrial mRNA by poly(A) specific ribonuclease is conserved among land plants

Running title: Marchantia PARN functions in mitochondria

Mai Kanazawa1*, Yoko Ikeda1,2*, Ryuichi Nishihama3, Shohei Yamaoka3, Nam Hee Lee4, Katsuyuki T. Yamato5, Takayuki Kohchi3, Takashi Hirayama1,2

1. Graduate School of Environment and Life Science, Okayama University. 2-20-1 Chuo, Kurashiki, 710-0046, Japan.
2. Institute of Plant Science and Resources, Okayama University. 2-20-1 Chuo, Kurashiki, 710-0046, Japan.
3. Graduate School of Biostudies, Kyoto University. Kitashirakawa Oiwake-cho, Sakyo-ku, Kyoto 606-8502, Japan
4. Department of Life Sciences, Faculty of Science and Engineering, Sorbonne University. 4 Place Jussieu 75005, Paris, France
5. Faculty of Biology-Oriented Science and Technology, Kindai University. 930 Nishimitani, Kinokawa, Wakayama 649-6493, Japan
*: Co-contributers.

Corresponding author:
Takashi Hirayama
Institute of Plant Science and Resources, Okayama University. 2-20-1 Chuo, Kurashiki, 710-0046, Japan.
e-mail: hira-t@okayama-u.ac.jp

Abstract

Regulation of the stability and the quality of mitochondrial RNA is essential for the maintenance of mitochondrial and cellular functions in eukaryotes. We have previously reported that the eukaryotic poly(A)-specific ribonuclease (PARN) and the prokaryotic poly(A) polymerase encoded by *AHG2* and *AGS1*, respectively, coordinately regulate the poly(A) status and the stability of mitochondrial mRNA in Arabidopsis. Mitochondrial function of PARN has not been reported in any other eukaryotes. In order to know how much this PARN-based mitochondrial mRNA regulation is conserved among plants, we studied the AHG2 and AGS1 counterparts of the liverwort, *Marchantia polymorpha*, a member of basal land plant lineage. We found that *M. polymorpha* has one ortholog each for *AHG2* and *AGS1*, named Mp*AHG2* and Mp*AGS1*, respectively. Their Citrine fused proteins were detected in mitochondria of the liverwort. Molecular genetic analysis showed that Mp*AHG2* is essential and functionally interacts with Mp*AGS1* as observed in Arabidopsis. A recombinant MpAHG2 protein had a deadenylase activity *in vitro*. Overexpression of Mp*AGS1* and the reduced expression of Mp*AHG2* caused an accumulation of polyadenylated Mp*cox1* mRNA. Furthermore, Mp*AHG2* suppressed Arabidopsis *ahg2-1* mutant phenotype. These results suggest that the PARN-based mitochondrial mRNA regulatory system is conserved in land plants.

Introduction

Regulation of gene expression is a fundamental system of life. Gene expression is controlled at various levels, namely at the transcriptional, post-transcriptional, translational, and post-translational levels. It has been widely accepted that RNA is one of the most important biological materials in the gene expression regulation. RNA itself has an ability to transfer genetic information from genomic DNA as translatable mRNA, to build functional structures alone or interacting with proteins, and to regulate gene expressions by means of micro RNAs (Filipowicz et al., 2008). Regarding the prominence of these RNAs, all the types of RNA molecules in the cell are believed to be under tight regulation at both their quantity and quality (Isken and Maquat, 2007; Houseley et al., 2006). Poly(A) sequence attached at the 3' end of RNA has a pivotal role in the RNA regulatory system. Poly(A) tail bound with poly(A) binding proteins constitutes the base for stable mRNA-protein complex composed with eIF4E and eIF4G (Wilkie et al., 2003; Goldstrohm and Wickens, 2008). Once poly(A) tail is shortened by deadenylases, RNA-protein complex becomes unstable and accessible by various RNases, and mRNA is degraded. On the other hand, poly(A) functions as a degradation tag for RNA in prokaryotes and functional RNAs such as tRNA or rRNAs in eukaryotes (Houseley et al., 2006).

Eukaryotes have, at least, three types of deadenylases, CCR4-NOT-CAF1 complex, PAN2-PAN3, and poly(A)-specific ribonuclease (PARN). The poly(A) status of cytoplasmic mRNA is mainly regulated by the CCR4-NOT-CAF1 and PAN2-PAN3 complexes (Chen and Shyu, 2011). PARN is widely distributed in eukaryotes but is not found in budding yeast and Drosophila. PARN was first reported to regulate the poly(A) status of maternal mRNA in Xenopus oocytes (Korner et al., 1998). Then, PARN has been shown to function in the poly(A) removal of various RNAs (Goldstrohm and Wickens, 2008; Weill et al., 2012; Norbury, 2013). More recent studies showed that animal PARN has a pivotal role in the maturation of functional RNAs such as small RNA, telomerase RNA component and ribosomal RNA (Berndt et al., 2012; Yoda et al., 2013; Moon et al., 2015; Stuart et al., 2015; Tang et al., 2016; Shukla et al., 2016; Ishikawa et al., 2017; Montellese et al., 2017; Shukla et al., 2019).

RNA in organelle is no exception. In plants, several steps comprise the mitochondrial post-transcriptional regulations. Mitochondrial transcripts undergo 5' and 3' end processing, splicing, RNA editing, and polyadenylation (Hammani and Giegé, 2014). Polyadenylation of

mitochondrial mRNA has been reported in various eukaryotes. However, its physiological role can be different among eukaryotes and is still controversial (Gagliardi et al., 2004). In human, polyadenylation was shown to stabilize some mitochondrial mRNAs but destabilize other mitochondrial mRNAs (Tomecki et al., 2004; Nagaike et al., 2008; Nagao et al., 2008) and described to be required for translation (Rorbach et al., 2011). In plant mitochondria, polyadenylation occurs at 3' termini, and average tail length was 22 nucleotides in maize (Lupold. et al., 1999). Polyadenylation of plant mitochondrial mRNA is believed to induce degradation of RNA as in bacteria, implying that the physiological role of polyadenylation in mitochondria has been conserved from the symbiotic alpha proteobacteria (Lange et al., 2009). Along with this idea, it has been thought that polyadenylation of plant mitochondrial mRNA is regulated by polynucleotide phosphorylase (PNPase). PNPase is a bifunctional enzyme possessing 3'-5' phosphorolytic exoribonuclease activity and 3'-terminal oligonucleotide polymerase activity. In *E. coli*, PNPase is responsible for the polyadenylation of mRNA (Mohanty and Kushner, 2010). Actually, reduced expression of a mitochondria-localized PNPase in Arabidopsis caused an accumulation of unprocessed polyadenylated *atp9* transcripts (Perrin et al., 2004).

Arabidopsis has a gene encoding PARN that is essential for embryogenesis and growth (Reverdatto et al., 2004; Chiba et al., 2004). We have been studying the function of this gene because its partially defective mutation, *ABA hypersensitive germination2-1* (*ahg2-1*), causes enhanced responses to abscisic acid and salicylic acid, plant hormones involved in environmental stress responses (Nishimura et al., 2005; Nishimura et al., 2009). We have reported previously that AHG2/AtPARN is localized to mitochondria and is involved in the regulation of poly(A) status of mitochondrial mRNA, counter-interacting with a bacterial type poly(A) polymerase (PAP), AGS1, which was identified as the *ahg2-1* suppressor mutant gene (Hirayama et al., 2013). Such the poly(A) regulation of mitochondrial mRNA has not been reported in animals or yeasts. This unique utilization of PARN and the regulation of the mitochondrial mRNA poly(A) status of Arabidopsis might reflect the distinct characteristics of plant cells which possess two different symbiotic organelles. However, it is not confirmed yet whether this AHG2-AGS1 system is conserved among plants or not, even though AHG2/PARN homologs are predicted to be localized to mitochondria in various plant species (Hirayama,

2014). To address this issue, we studied AHG2 and AGS1 counterparts in a liverwort, *Marchantia polymorpha*, a member of a basal land plant lineage (Bowman et al., 2007; Bowman et al., 2017). We demonstrated that both the *M. polymorpha* counterparts of AHG2 and AGS1 are localized to mitochondria and functionally interact with each other, and that the poly(A) status and the levels of mitochondrial mRNA were affected by the genetic modulation of Mp*AHG2* and Mp*AGS1*. Our data suggest that the AHG2 and AGS1 system where a PARN and a PAP regulate the poly(A) status of mitochondrial mRNA is conserved among land plants.

Results

Identification of Arabidopsis *AHG2* and *AGS1* orthologs in the *M. polymorpha* genome.

To identify the *M. polymorpha* orthologs of Arabidopsis *AHG2* and *AGS1*, transcripts with a potential to encode proteins similar to these Arabidopsis proteins were searched against *M. polymorpha* EST and full-length cDNA databases along with the genome sequence data. We successfully identified the candidates with higher similarities in amino acid sequences to Arabidopsis AHG2 and AGS1 (hereafter mentioned as AtAHG2 and AtAGS1, respectively). According to the genome sequence data (*M. polymorpha* JGI version 3.1, Bowman et al., 2017), *M. polymorpha* has one ortholog each for *AtAHG2* and *AtAGS1* (Supplementary Figure S1, S2). We then named these orthologs Mp*AHG2* (gene ID: Mapoly0076s0056.1) and Mp*AGS1* (gene ID: Mapoly0136s0037.1 and Mapoly0171s0002.1) according to the nomenclature (Bowman et al., 2016), respectively, and focused on them in this study.

A phylogenetic analysis showed that Arabidopsis and several other plants have additional AHG2/PARN homologs, although these amino acid sequences are less conserved and constitute an additional clade (Supplementary Figure S1). Among animal PARNs, R3H and RNA recognition (RRM) motifs are highly conserved (Wu et al., 2009). These motifs are not found in MpAHG2 and other plant PARN homologs (Supplementary Figure S2A), but the amino acid sequences of the corresponding positions for these motifs are highly conserved among plant PARNs, implying that these portions are required for the function of plant PARNs. Bacterial type PAP shares the amino acid sequence with CCA-adding enzyme, which adds triplet C-C-A residues to the 3'end of tRNA creating the amino acid accepting structure. Both enzymes belong to terminal nucleotidyltransferase, but these can be distinguished by the

presence or absence of the PAP-specific motifs (Martin and Keller, 2004). According to this classification, MpAGS1 belongs to the PAP family (Supplementary Figure S2B). Consistently, a phylogenetic analysis also showed that Arabidopsis At1g22660, which was previously shown to be a CCA adding enzyme (Zimmer et al., 2009), is distant from MpAGS1 and AtAGS1 (Supplementary Figure 2B).

MpAHG2- and MpAGS1-Citrine fusion proteins are localized to mitochondria in *M. polymorpha* cells.

In order to determine the subcellular localizations of MpAHG2 and MpAGS1, open reading frames of Mp*AHG2* and Mp*AGS1* cDNA clones were translationally fused with a Citrine gene and placed under the constitutive 35S promoter. These recombinant genes were introduced into *M. polymorpha* cells and several stable transgenic lines were established. Under a laser-scanning microscope, wild-type cells showed very weak fluorescence of chloroplasts which most probably depending on auto fluorescence, while Citrine fluorescence was detected clearly in both the MpAHG2-Citrine and MpAGS1-Citrine transgenic lines (Figure 1). In both lines, the Citrine fluorescence was detected as spots dispersed in the cell. When the tissues were stained with MitoTracker, the Citrine signals were almost completely overlapped with MitoTracker signals, suggesting that MpAHG2 and MpAGS1 are localized to mitochondria of *M. polymorpha*.

Attempts to obtain the loss-of-function mutants of Mp*AHG2*.

To understand the physiological roles of MpAHG2, we made an attempt to obtain Mp*AHG2* disruption mutants using the homologous recombination mutagenesis. However, no such the mutants were obtained after analyzing more than 500 antibiotic resistant lines, while the general efficiency of mutant isolation by homologous recombination is about 2% in *M. polymorpha* (Ishizaki et al., 2013). This result suggests that Mp*AHG2* is essential for survival in *M. polymorpha,* similar to *AtAHG2* in Arabidopsis. Therefore, we used the CRISPR/Cas9 mutagenesis expecting to introduce more moderate mutations such as an amino acid substitution. We chose five target sequences; two for exons and three for exon-intron junctions (Figure 2A). Using these targets, consequently, three independent mutants (Mp*ahg2-1*,

Mp*ahg2-2*, and Mp*ahg2-3*) were obtained and all were edited near the junction of the second intron and the third exon. In these mutant lines, several nucleotides at six or seven bases upstream of the intron-exon junction were deleted (Figure 2B). Interestingly, these three mutant candidates showed a retarded growth with different extent; Mp*ahg2-1* showed the strongest and Mp*ahg2-3* showed the weakest phenotypes (Figure 2C, Supplementary Figure S3). The transcript levels of Mp*AHG2* in these lines were decreased to some extent (Figure 2D) and seemed to correlate with the retarded growth phenotypes (Figure 2C, 2D). The nucleotide sequence of Mp*AHG2* cDNA obtained from these mutants were identical to the 'CUFF' transcript data in MarpolBase database (http://marchantia.info) indicating that the intron was removed normally. These results imply that the few-base deletion near the junction of second intron and third exon reduced the expression of Mp*AHG2* which caused the growth retardation phenotype, and further suggest that Mp*AHG2* is indispensable for the growth of *M. polymorpha*.

Isolation of the loss-of-function mutants of Mp*AGS1*.

To address the physiological roles of Mp*AGS1*, we also made the loss-of-function mutants of this gene. The CRISPR/Cas9 constructs that harbored a guide RNA targeting Mp*AGS1* exon 5 (target1 or target2) were introduced into *M. polymorpha* cells and transgenic lines were obtained (Figure 3A). Among them, we successfully obtained two independent mutants, Mp*ags1-1* or Mp*ags1-2*, which had 1 bp insertion or 7 bp deletion causing a frame-shift and premature translation termination of Mp*AGS1*, respectively (Figure 3B). Both of the mutants exhibited weak growth-retardation phenotypes under normal growth conditions (Figure 3C). The fresh weights of the thallus of the Mp*ags1* mutants were about 65% of that of wild type (Figure 3D). These data indicate that Mp*AGS1* is dispensable but required for normal growth of *M. polymorpha*.

Isolation of Mp*ahg2* Mp*ags1* double mutants.

In Arabidopsis, loss-of-function mutations of the *AtAGS1* gene suppressed the lethality of the *AtAHG2* disruption mutant (Hirayama et al., 2013). If there is a similar genetic interaction between Mp*AHG2* and Mp*AGS1*, loss-of-function mutations of Mp*AHG2* can be obtained in the Mp*ags1* defective mutation background. The CRISPR/Cas9 constructs with the target

sequence for the first exon (target1) or the last exon (target2) of Mp*AHG2* (Figure 2A), with which we had failed to obtain mutants in the wild-type background as described above, were introduced into the Mp*ags1-1* and Mp*ags1-2* lines. Intriguingly, with this approach, several loss-of-function mutations of Mp*AHG2* were successfully obtained. Among them we chose three lines, Mp*ags1-1*Mp*ahg2-4*, Mp*ags1-1*Mp*ahg2-5*, and Mp*ags1-2*Mp*ahg2-6* (Figure 4A, Supplementary Figure S4). All of the identified mutations had insertions in the exon causing a frame shift and premature translation termination of Mp*AHG2*. Their growth rates were lower compared to that of wild type but were similar to those of Mp*ags1-1* or Mp*ags1-2* (Figure 4B, C). These observations suggest that the lethality of loss-of-function mutation of Mp*ahg2* is suppressed by the mutations of Mp*AGS1*, and that Mp*ahg2* and Mp*ags1* have a genetic interaction.

Biochemical properties of MpAHG2 and MpAGS1.

To characterize MpAHG2 and MpAGS1 proteins, their *in vitro* biochemical activities were examined. For this purpose, recombinant proteins were produced and isolated (Supplementary Figure S5). Using these recombinant proteins, *in vitro* activities were assayed. To examine the deadenylase activity of the recombinant MpAHG2, various substrate RNAs were prepared (Figure 5A) and co-incubated with the recombinant protein, and then their lengths were analyzed with capillary electrophoresis (Figure 5B). When poly(A)$_{25}$ and poly(A)$_{18}$ RNA, in which 25 nt and 18 nt poly(A) sequences were added to a 56 nt vector sequence, respectively, were incubated with the recombinant MpAHG2, the signals corresponding to the full-length RNAs of poly(A)$_{25}$ and poly(A)$_{18}$ were disappeared but instead a signal corresponding to the vector sequence was appeared. When poly(U)$_{25}$ RNA was used, signals corresponding to the intact substrate RNA and various fragments with larger molecular weight than 56 nt were observed. And a clear substrate shortening was not observed when the vector sequence RNA was used. These data suggest that the recombinant MpAHG2 alone has the ability to remove poly(A) sequence preferentially from RNA substrates *in vitro*, confirming that MpAHG2 belongs to the poly(A)-specific ribonuclease.

Similarly, the PAP activity of the recombinant MpAGS1 was assessed using these RNA substrates. However, we were not able to detect the PAP activity even though various

experimental conditions, such as buffer pH or nucleotide tri-phosphate composition, were changed. Previously under the same *in vitro* assay conditions, we could successfully detect the AtAGS1 activity (Hirayama et al., 2013). Therefore, it implied that the purified recombinant MpAGS1 protein alone does not have the PAP activity.

Poly(A) status of mitochondrial mRNA in Mp*AGS1*-overexpression and Mp*ahg2* mutant *M. polymorpha* lines.

To address the PAP activity of MpAGS1 *in vivo*, we produced transgenic *M. polymorpha* lines possessing a recombinant gene in which Mp*AGS1* cDNA was fused to 35S promoter. These lines showed a slightly retarded growth phenotype (Supplementary Figure S6A). The increased Mp*AGS1* transcript levels were confirmed by qRT-PCR experiments (Supplementary Figure S6B). We examined the poly(A) status of steady-state mitochondrial Mp*cox1* mRNA of these lines was analyzed with poly(A)-tail (PAT) assay that amplifies the cDNA for the poly(A) tail attached at the 3' end of the target gene mRNA. Interestingly, an additional and more intense PAT product was detected in the Mp*AGS1* overexpression lines (Figure 6A). Sequencing analysis of these DNA fragments revealed that these PAT products actually were derived from polyadenylated Mp*cox1* mRNA (Figure 6B). These data strongly suggest that MpAGS1 is involved in poly(A) addition in the liverwort mitochondria. With the same experimental approach, poly(A) status of mitochondrial mRNA in the Mp*ahg2* mutant lines, severe mutant Mp*ahg2-1* and moderate mutant Mp*ahg2-2*, were examined. As shown in Figure 6A, the additional DNA fragments with almost the same molecular length observed in the Mp*AGS1*-overexpression lines were detected. The signal intensity of this DNA fragment was stronger in the severe mutant Mp*ahg2-1* than in the moderate mutant Mp*ahg2-2*. The DNA fragment isolated from Mp*ahg2-1* sample also possessed a poly(A) sequence (Figure 6B).

In our previous study with Arabidopsis, we demonstrated that the *Atahg2-1* mutation increases the mitochondrial mRNA levels (Hirayama et al., 2013). Then we next examined how the defect of Mp*AGS1* or Mp*AHG2* or the overexpression of Mp*AGS1* affects the mitochondrial mRNA levels. As shown in Figure 7, in the severe Mp*ahg2-1* mutant, the transcript levels of all of the mitochondrial gene examined were increased, more or less. The genetic modulation of Mp*AGS1* also affected the transcript levels of mitochondrial genes. The transcript levels of

Mp*cob*, Mp*nad1,* and Mp*atp9* were significantly increased in the Mp*ags1-2* defective mutant while they were not affected consistently in the Mp*AGS1*-overexpression lines (Figure 7). By contrast, the transcript levels of Mp*cox1*, Mp*nad5*, and Mp*atp8* were slightly increased in Mp*ags1-2* while they were apparently decreased in the Mp*AGS1*-overexpression lines. These data imply that an enhanced MpAGS1 activity tends to decrease the mitochondrial transcript levels. Consistently, reduced activity of MpAGS1 in Mp*ags1* tends to increase the mitochondrial mRNA levels.

The transcript levels of Mp*AGS1* and Mp*AHG2* were also examined. The Mp*AHG2* transcripts were slightly less accumulated in the Mp*AGS1*-overexpression lines and Mp*ags1-2*. On the other hand, the Mp*AGS1* transcripts were slightly increased in Mp*ahg2-1* (Supplementary Figure S6B). These observations suggest that the activities of MpAGS1 and MpAHG2 affect the expression of Mp*AHG2* and Mp*AGS1*, respectively, although its mechanism and physiological relevance are unknown. It is obvious that the affected expression of Mp*AGS1* in Mp*ahg2-1* or Mp*AHG2* in the Mp*AGS1*-overexpression lines and Mp*ags1-2* were not the cause of the altered expression of mitochondrial genes because there is no clear correlation.

Complementation analysis of Arabidopsis mutant by *M. polymorpha* genes.

All the data described above suggest that MpAHG2 and MpAGS1 function in *M. polymorpha* mitochondria as AtAHG2 and AtAGS1 do in Arabidopsis mitochondria, respectively. To confirm this idea, we asked if Mp*AHG2* or Mp*AGS1* behaves as AtAHG2 or AtAGS1 does in Arabidopsis, respectively. The recombinant Mp*AHG2* or Mp*AGS1* cDNA, in which the N-terminal portion predicted as a transit peptide for mitochondrial localization was replaced with the signal peptide of an Arabidopsis mitochondria-localized protein PNPase (At5g14580). When the recombinant Mp*AHG2* cDNA clone was introduced into the Arabidopsis *ahg2-1* mutant, the dwarf phenotype of *ahg2-1* was partially suppressed regarding the size of the rosette (Figure 8A, Supplementary Figure S7A). A PAT assay for Arabidopsis mitochondria *cox1* or *nad7* mRNAs revealed that the amounts of polyadenylated mRNA and total mRNA for these genes were significantly decreased in the *ahg2-1* transgenic plants expressing Mp*AHG2* (Figure 8B, 8C), consistent with the morphological phenotype. The poly(A) status of Arabidopsis

mitochondria *orf107* mRNA was examined by cRT-PCR assay. In *Atahg2-1,* polyadenylated clones (additional A residues, more than two) were detected in 18 of 34 clones examined (Hirayama et al., 2013). In the Mp*AHG2* transgenic line #1, only 5 of 33 clones examined were polyadenylated (Supplementary Table S1). These data indicate that Mp*AHG2* has ability to compensate the defect of the *ahg2-1* mutation of Arabidopsis. Increased AGS1 activity in Arabidopsis would confer the *Atahg2-1*-like phenotype *in planta*, namely a dwarf phenotype, and accumulate polyadenylated *Atnad7* in cells (Hirayama et al., 2013). We obtained a few transgenic lines expressing recombinant Mp*AGS1* gene in the wild-type background. However, these transgenic lines did not show any visible phenotypes (Supplementary Figure S7B). Consistently, we could detect only faint PAT fragments of *Atnad7* and *Atcox1* in MpAGS1 overexpressing lines (Figure 8B).

Discussion

In Arabidopsis, the stability of mitochondrial mRNA seems to be regulated through 3' end polyadenylation and deadenylation by AtAGS1/PAP and AtAHG2/PARN, respectively (Hirayama et al., 2013). In this study we showed that a liverwort, *M. polymorpha*, which is a member of a basal land plant lineage, has a mitochondrial polyadenylation system similar to that of Arabidopsis. This conclusion is supported by our data showing that MpAGS1 and MpAHG2 encoded by the *AtAGS1* and *AtAHG2* orthologous genes, respectively, (Supplementary Figure S1) were localized to mitochondria of *M. polymorpha* (Figure 1), that MpAHG2 had a deadenylase activity *in vivo* and *in vitro* (Figure 5, 6, 8), and that MpAGS1 had a PAP activity *in vivo* (Figure 6). And most importantly, the lethality of the Mp*AHG2* loss-of-function mutation was suppressed by the Mp*AGS1* loss-of-function mutation (Figure 2, 4), suggesting that MpAHG2 and MpAGS1 regulate the same RNA substrates. We also demonstrated that the heterologous expression of Mp*AHG2* complemented, at least partly, *Atahg2-1* in Arabidopsis. It is plausible that the AGS1/PAP-AHG2/PARN regulatory system is conserved among land plants.

However, there are several different properties between the Arabidopsis and *M. polymorpha* AHG2-AGS1 systems. First, although the Arabidopsis *AtAGS1* defective mutants did not exhibit any clear visible phenotypes (Hirayama et al., 2013), the Mp*ags1* mutants

displayed weak growth retardation (Figure 3). This finding implies that poly(A) addition of mitochondrial mRNA is physiologically more important in *M. polymorpha* than Arabidopsis. Alternatively, it is possible that MpAGS1 has additional roles. Secondly, the recombinant MpAGS1 proteins did not show polyadenylase activity at all in the experimental conditions where a recombinant AtAGS1 protein could. Considering the high similarity of amino acid sequence between MpAGS1 and AtAGS1, the molecular phenotype of mitochondrial mRNA in the Mp*AGS1* overexpressing *M. polymorpha* lines, and the genetic interaction between the Mp*ags1* and Mp*ahg2* defective mutants, it is more plausible that MpAGS1 has a polyadenylase activity. We tried to detect the activity of a recombinant MpAGS1 protein by changing experimental conditions but failed. On the other hand, we could detect a strong deadenylase activity of the recombinant MpAHG2 protein whereas we had not been able to detect the AtAHG2 activity in the same conditions. These observations had led us to an idea that AtAGS1 and MpAHG2 can exhibit their enzymatic activities alone whereas MpAGS1 and AtAHG2 require other components or post-translational modifications for their activities. The absence of strong molecular phenotypes in the transgenic Arabidopsis expressing Mp*AGS1* is consistent with this idea (Figure 8B, 8C). Identification of the co-factors for MpAGS1 and AtAHG2 will lead us to the comprehension of uniqueness of plant mitochondria and plants.

Poly(A)-specific ribonuclease (PARN) is distributed widely in eukaryotes and has been reported to be involved in the poly(A) removal of various RNAs (Goldstrohm and Wickens, 2008; Weill et al., 2012; Norbury, 2013). Recent studies of PARN in animals showed that PARN has a pivotal role in the maturation of non-protein coding functional RNA such as small RNA, telomerase RNA component and ribosomal RNA (Berndt et al., 2012; Yoda et al., 2013; Moon et al., 2015; Stuart et al., 2015; Tang et al., 2016; Shukla et al., 2016; Ishikawa et al., 2017; Montellese et al., 2017; Shukla et al., 2019). In this study on *M. polymorpha* MpAHG2 and our previous study on Arabidopsis AtAHG2, we demonstrated these plant PARNs were predominantly localized to mitochondria. Although we cannot exclude the possibility that plant PARNs are involved in the RNA processing in the nucleus or cytoplasm as animal PARNs do, molecular phenotypes of Arabidopsis mutants, *M. polymorpha* mutants, or transgenic lines are consistent with the mitochondrial function of thses PARNs. In organisms lacking PARN, such as budding yeast and Drosophila, other factors are involved in the

processing of functional RNA molecules in which animal PARNs are implicated. Plants might have similar alternative regulations.

Amino acid sequences of PARNs are highly conserved among vertebrates (Godwin et al., 2013). These animal PARNs have two conserved domains, R3H and RRM (Supplementary Figure S1). These motifs are required for binding to the 5'-CAP structure of mRNA (Nilsson et al., 2007; Wu et al., 2009). The CAP-binding activity of PARN is thought to be necessary for the regulation of poly(A) status of mRNA. Interestingly, plant PARNs are lacking these motifs. This distinct structure of plant PARN implies their different biochemical function. As we demonstrated with AtAHG2 and MpAHG2, plant PARNs are localized and function in mitochondria, CAP binding activity is not necessary for them since mitochondrial mRNA lacks the CAP structure.

There have been arguments on the relationships among the processes of poly(A) addition, poly(A) removal, and degradation of mRNA. Presumably a reduced expression of Mp*AHG2* and an increase expression of Mp*AGS1* would cause the same effect because either modulation results in the accumulation of polyadenylated mitochondrial mRNA. In this study, we showed that the Mp*ahg2-1* mutation resulted in the accumulations of both polyadenylated and total mRNA of several mitochondrial genes (Figure 6, 7), as observed in the Arabidopsis *ahg2-1* mutant (Hirayama et al., 2013). We also showed that the overexpression of Mp*AGS1* in *M. polymorpha* increased polyadenylated mRNAs. However, the transcript levels of mitochondrial genes were lower accumulated in the Mp*AGS1*-overexpressing lines while those were higher in the Mp*ags1* mutant. This discrepancy can be explained by the presence or absence of MpAHG2. The polyadenylated mRNA in the Mp*AGS1*-overexpressing lines would be the target of poly(A) removal by MpAHG2 and the subsequent RNA degradation. Thus the increased ratio of polyadenylated mRNA would induce the degradation of mRNA and result in the decrease of the total mRNA levels in the presence of AHG2/PARN. Our observations in this study and previous study support the idea that the removal of poly(A) of plant mitochondrial mRNA induces the degradation of mRNA.

Plant and animal mitochondria have been thought to share many characteristics. However, detailed analyses have revealed that they are quite different from each other. Animal mitochondrial genome is about 15-20 kb in length and containing less than 37 genes (including

tRNA genes) (Boore, 1999). In human mitochondria, each strand of mitochondrial DNA is transcribed as a single transcript and then processed to several mRNAs (Mercer et al., 2011). By contrast, mitochondrial genomes of *M. polymorpha* and Arabidopsis are about 186 kb and 370 kb in length, respectively, and both genomes contain about 60 genes (Oda et al., 1992; Unseld et al., 1997). Most of their protein-coding genes seem to be transcribed separately. Such differences in gene number and transcript structures might require distinct regulatory mechanisms. One possible explanation for this plant uniqueness is that plant cells have another symbiotic organelle, plastid. It can be postulated that, in the evolutionary process, plants needed a specific gene regulatory system for each symbiotic organelle. During such a process, PARN might have been appointed to the mitochondrial specific mRNA regulator. Interestingly, algae do not seem to possess this AGS1-AHG2 system. Chlamydomonas does not have PARN (Zimmer et al., 2008). Recent study showed that mitochondrial mRNA is polycytidylated in Chlamydomonas (Salinas-Giegé et al., 2017), indicating that this alga has different strategies to regulate mitochondrial mRNA. It might be possible that the AGS1-AHG2 system was required to adapt to the terrestrial environment when plants landed during the evolution. This idea is consistent with the fact that *Atahg2-1* has environmental stress-related phenotypes (Nishimura et al., 2005; Nishimura et al., 2009; Hirayama et al., 2018). Further analysis on the plant specific mitochondrial regulation will offer us clues to understand the unique and elaborated system of plants to cope with environment stresses.

Materials and Methods

M. polymorpha growth conditions

Marchantia polymorpha Takaragaike-1 (Tak-1, male accession) and Takaragaike-2 (Tak-2, female accession) were used as wild-type plants (Ishizaki et al., 2008). *M. polymorpha* was cultured asexually under continuous white light at 22 °C. F1 spores generated by crossing Tak-2 and Tak-1 were used for transformation. Mature sporangia were collected 3–4 weeks after crossing, air-dried for 7–10 days and stored at –80°C until use.

Phylogenetic analysis

Protein or transcript sequences were obtained by the BLAST search against Arabidopsis AHG2

and AGS1 in JGI Phytozome V12.2 (https://phytozome.jgi.doe.gov/pz/portal.html) for Viridiplantae lineage and in the GenBank databases at NCBI for *Homo sapiens* and *Xenopus laevis*. Multiple sequence alignments were performed using the MUSCLE program (Edgar, 2004) contained in the Geneious ver.11.1.3 package with the default settings, and at least 20% alignment gaps were automatically removed by using the mask alignment function in the Geneious package. After removing alignment gaps, trees were constructed using the fast maximum likelihood tree estimation program PhyML using the LG amino acids replacement matrix (Guindon and Gascuel, 2003). Bootstrap proportions were computed from 1000 trials.

Constructing transgenic *M. polymorpha*

cDNAs of Mp*AHG2* or Mp*AGS1* were amplified by PCR using cDNA mixture prepared from wild type (Tak-1) total RNA with gene specific primers (Supplementary Table S2). These cDNAs were cloned in pDONR207 and the nucleotide sequence was confirmed. For constructing transgenic *M. polymorpha* expressing MpAHG2 or MpAGS1, cDNA clones were inserted into pMpGWB202 under the cauliflower mosaic virus-derived constitutive 35S promoter (Ishizaki et al., 2015). For constructing transgenic *M. polymorpha* expressing MpAHG2- or MpAGS1-Citrine fusion protein, Mp*AHG2* or Mp*AGS1* cDNA without terminal codon was inserted into pMpGWB106 under 35S promoter (Ishizaki et al., 2015). These recombinant plasmids were transferred to F1 sporelings or mutant thallus using *Agrobacterium tumefaciens* GV3101 strain with the method previously described (Ishizaki et al., 2008; Kubota et al., 2013). Transformants were selected on half-strength B5 agar medium containing 1% agar, appropriate antibiotics (10 mg/L hygromycin, 100 mg/L gentamicin, and 0.5μM chlorsulfuron, respectively), and 100 mg /L cefotaxime (Claforan: Sanofi-Aventis).

Mutant construction

All the *M. polymorpha* mutants in this study were obtained by CRISPR/Cas9 system optimized for *M. polymorpha* by Sugano et al. (Sugano et al., 2014; Sugano et al., 2018). Double strand oligo DNAs corresponding to each single guide RNA (sgRNA) target regions (Supplementary Table S2) was inserted into the *Bsa*I site in the downstream of U6 promoter of pMpGE_En03 vector according to the procedure described previously (Ikeda et al., 2018). Resultant plasmids

were recombined with pMpGE010 or pMpGE011 binary vector and used for transformation with *Agrobacterium*.

Constructing transgenic Arabidopsis expressing Mp*AHG2* and Mp*AGS1*

To express MpAHG2 or MpAGS1 in Arabidopsis, recombinant Mp*AHG2* and Mp*AGS1* genes in which their putative mitochondrial target signal sequences were replaced with that of an Arabidopsis mitochondria-localized protein gene (At5g14580) were constructed. These recombinant genes were placed under 35S promoter of a binary vector and used to transform Arabidopsis via *Agrobacterium* with the floral dip methods (Clough and Bent, 1998).

Quantitative real-time PCR experiments

For *M. polymorpha* samples, total RNA was isolated from plants grown from gemmae for 30-40 days on half-strength B5 medium containing 1% sucrose and 1% agar with RNAzol (Molecular Research Center, Inc.) according to the manufacture's instruction. For Arabidopsis samples, total RNA was isolated from two-week-old plants using Qiagen RNeasy Plant Mini Kit (Qiagen). 1 µg of total RNA was treated with RNase free DNase (Promega), and then used for cDNA synthesis using PrimeScript II 1st strand cDNA Synthesis Kit with random primers (Takara Bio Inc.). Quantitative real-time PCR was performed on a LightCycler 96 System (Roche Diagnostics) in a total volume of 20 µL containing 10 µL TB Green Primer Ex Taq II (Takara Bio Inc.), 8 pmol each primer, and a cDNA mixture described above using gene specific primers (Supplementary Table S2). The amplification program consisted of 40 cycles of 95 °C for 10 s and 60 °C for 1 min. To calculate the relative amount transcripts, the comparative Ct method was used.

Poly(A) tail assay and cRT-PCR

Total RNA was isolated from two-week-old Arabidopsis plants using Qiagen RNeasy Plant Mini Kit (Qiagen) and used for cDNA synthesis with a $dT(15)^{+}$-T7 promoter sequence primer. Poly(A) tail (PAT) assays were performed using a cDNA mixture with the T7 primer and a gene-specific primer for the sequence near the 3'-end of mRNA (Supplementary Table S2). The reaction mixture was analyzed with an Agilent 2100 Bioanalyzer. The procedures for

circularization-RT-PCR (cRT-PCR) were derived from Couttet et al. (Couttet et al., 1997). Arabidopsis *orf107f* gene-specific cRTR1 primers were used for cDNA synthesis after RNA circularization and gene-specific cRTF and cRTR2 primers were used for PCR (Supplementary Table S2).

In vitro assay

Recombinant proteins were produced using the TNT SP6 high yield wheat germ protein expression system (Promega) with Halo-tag fused genes harbored by pFN19K vector, and Halo-tagged recombinant proteins were purified using the Halo-tag binding resin. After the digestion with a sequence specific protease, recombinant protein without Halo-tag moiety was purified. To detect the recombinant protein with western blotting, purified proteins were separated on an SDS-PAGE gel and then transferred to a PVDF membrane and exposed to anti-MYC-epitope-tag antibody (1:2000, Nakalai Tesque). The primary antibody was detected with a peroxidase-labeled anti-mouse-antibody (1:1000, GE Healthcare). Substrate RNA was synthesized using pGEM4z vector as described by Reverdatto et al. (Reverdatto et al., 2004; Supplementary Table S2). Substrate RNA (0.4 μg) and recombinant proteins (~20 ng) were mixed and incubated in a buffer (10 mM HEPES pH 7.2, 50 mM KCl, 5 mM $MgCl_2$, 1 mM DTT, 0.25 mM each ribonucleotide, total volume 10 μL) at 23 °C for 1 h. A portion (1 μL) of the reaction mixture was analyzed using an Agilent Small RNA kit (Agilent Technologies) with an Agilent 2100 Bioanalyzer.

Microscopic observation

To visualize mitochondria, plant materials were stained with 150 nM MitoTracker Red CMXRos (Life Technologies Corporation) for 30 min at room temperature and washed with water for 30 min. Fluorescence of Citrine or MitoTracker was observed under a confocal microscope (FV1000-D; Olympus). Staining and observation conditions were based on Minamino et al. (Minamino et al., 2018).

Supplementary data

Table S1. The results of circular RT-PCR assay for *AtORF107f* of *Atahg2-1* transgenic line

expressing Mp*AHG2*.

Table S2. List of oligonucleotides used in this study.

Figure S1. Rooted phylogenetic trees of MpAHG2 (A), MpAGS1 (B), and their related proteins in eukaryotes.

Figure S2. Alignments of amino acid sequences of MpAGS1, MpAHG2 and their homologs in plants.

Figure S3. Growth of the Mp*ahg2-1,* Mp*ahg2-2* and Mp*ahg2-3.*

Figure S4. Mutation of the Mp*ahg2-6* mutant.

Figure S5. Detection of recombinant MpAGS1 and MpAHG2 proteins.

Figure S6. The Mp*AGS1* overexpression lines.

Figure S7. Rosette leaf areas of Arabidopsis lines.

Acknowledgements

We thank Dr. Ryo Matsushima for his supporting in the experiments using the laser microscope, TH lab members for their technical supports, and Dr. Takehiko Kanazawa and Dr. Takashi Ueda for sharing their methods to stain *M. polymorpha* mitochondria with MitoTracker. N.-H. Lee is grateful to the mobility programs running between Sorbonne and Okayama universities.

Funding

This work was supported by Grant-in-Aid for Scientific Research, 15547992 and 19K22434 to TH from MEXT Japan.

Conflict of interest statement. None declared.

Author contribution

T.H., Y.I., and M.K. planned and designed the research. M.K., Y.I., N.-H.L and T.H. performed most of experiments. R.N., S.Y., and T.K. provided useful materials and information for experiments using liverwort. K.T.Y. provided important information on transcript levels in the *M. polymorpha* mutants used in this study. T.H., Y.I., R.N., S.Y., K.T.Y., and T.K. wrote the manuscripts. M.K. and Y.I. contributed equally.

Conflict of interest

The authors disclose any financial interests or connections, direct or indirect, or other situations that might raise the question of bias in the work reported or the conclusions, implications, or opinions stated - including pertinent commercial or other sources of funding for the individual author(s) or for the associated department(s) or organization(s), personal relationships, or direct academic competition.

References

Berndt, H., Harnisch, C., Rammelt, C., Stöhr, N., Zirkel, A., Dohm, J.C., et al. (2012). Maturation of mammalian H/ACA box snoRNAs: PAPD5-dependent adenylation and PARN-dependent trimming. *RNA* 18: 958–972.

Boore, J.L. (1999). Animal mitochondrial genomes. *Nucleic Acids Res.* 27: 1767–1780.

Bowman, J.L., Araki, T., Arteaga-Vazquez, M.A., Berger, F., Dolan, L., Haseloff, J., et al. (2016). The Naming of Names: Guidelines for Gene Nomenclature in Marchantia. *Plant Cell Physiol.* 57: 257–261.

Bowman, J.L., Floyd, S.K., and Sakakibara, K. (2007). Green Genes—Comparative Genomics of the Green Branch of Life. *Cell* 129: 229–234.

Bowman, J.L., Kohchi, T., Yamato, K.T., Jenkins, J., Shu, S., Ishizaki, K., et al. (2017). Insights into Land Plant Evolution Garnered from the Marchantia polymorpha Genome. *Cell* 171: 287-304.e15.

Chen, C.-Y.A. and Shyu, A.-B. (2011). Mechanisms of deadenylation-dependent decay. *Wiley Interdiscip. Rev. RNA* 2: 167–183.

Chiba, Y., Johnson, M.A., Lidder, P., Vogel, J.T., Erp, H. van, and Green, P.J. (2004). AtPARN is an essential poly(A) ribonuclease in Arabidopsis. *Gene* 328: 95–102.

Clough, S.J. and Bent, A.F. (1998). Floral dip: a simplified method for Agrobacterium - mediated transformation of Arabidopsis thaliana. *Plant J.* 16: 735–743.

Couttet, P., Fromont-Racine, M., Steel, D., Pictet, R., and Grange, T. (1997). Messenger RNA deadenylylation precedes decapping in mammalian cells. *Proc. Natl. Acad. Sci.* 94: 5628–5633.

Edgar, R.C. (2004). MUSCLE: multiple sequence alignment with high accuracy and high throughput. *Nucleic Acids Res.* 32: 1792–1797.

Filipowicz, W., Bhattacharyya, S.N., and Sonenberg, N. (2008). Mechanisms of post-transcriptional regulation by microRNAs: are the answers in sight? *Nat. Rev. Genet.* 9: 102–

114.
Gagliardi, D., Stepien, P.P., Temperley, R.J., Lightowlers, R.N., and Chrzanowska-Lightowlers, Z.M.A. (2004). Messenger RNA stability in mitochondria: different means to an end. *Trends Genet.* 20: 260–267.
Godwin, A.R., Kojima, S., Green, C.B., and Wilusz, J. (2013). Kiss your tail goodbye: The role of PARN, Nocturnin, and Angel deadenylases in mRNA biology. *Biochim. Biophys. Acta BBA - Gene Regul. Mech.* 1829: 571–579.
Goldstrohm, A.C. and Wickens, M. (2008). Multifunctional deadenylase complexes diversify mRNA control. *Nat. Rev. Mol. Cell Biol.* 9: 337–344.
Guindon, S. and Gascuel, O. (2003). A simple, fast, and accurate algorithm to estimate large phylogenies by maximum likelihood. *Syst. Biol.* 52: 696–704.
Hammani, K. and Giegé, P. (2014). RNA metabolism in plant mitochondria. *Trends Plant Sci.* 19: 380–389.
Hirayama, T. (2014). A unique system for regulating mitochondrial mRNA poly(A) status and stability in plants. *Plant Signal. Behav.* 9: e973809.
Hirayama, T., Matsuura, T., Ushiyama, S., Narusaka, M., Kurihara, Y., Yasuda, M., et al. (2013). A poly(A)-specific ribonuclease directly regulates the poly(A) status of mitochondrial mRNA in Arabidopsis. *Nat. Commun.* 4: 2247.
Houseley, J., LaCava, J., and Tollervey, D. (2006). RNA-quality control by the exosome. *Nat. Rev. Mol. Cell Biol.* 7: 529–539.
Hirayama, T., Lei, G.J., Yamaji, N., Nakagawa, N., Ma, J.F. (2018). The putative peptide gene FEP1 regulates iron deficiency response in Arabidopsis. *Plant Cell Physiol.* 59: 1739–1752.
Ikeda, Y., Nishihama, R., Yamaoka, S., Arteaga-Vazquez, M.A., Aguilar-Cruz, A., Grimanelli, D., et al. (2018). Loss of CG methylation in *Marchantia polymorpha* causes disorganization of cell division and reveals unique DNA methylation regulatory mechanisms of non-CG methylation. *Plant Cell Physiol.* 59: 2421-2431.
Ishikawa, H., Yoshikawa, H., Izumikawa, K., Miura, Y., Taoka, M., Nobe, Y., et al. (2017). Poly(A)-specific ribonuclease regulates the processing of small-subunit rRNAs in human cells. *Nucleic Acids Res.* 45: 3437–3447.
Ishizaki, K., Chiyoda, S., Yamato, K.T., and Kohchi, T. (2008). Agrobacterium-Mediated Transformation of the Haploid Liverwort Marchantia polymorpha L., an Emerging Model for Plant Biology. *Plant Cell Physiol.* 49: 1084–1091.
Ishizaki, K., Johzuka-Hisatomi, Y., Ishida, S., Iida, S., and Kohchi, T. (2013). Homologous recombination-mediated gene targeting in the liverwort *Marchantia polymorpha* L. *Sci. Rep.*

3: 1532.
Ishizaki, K., Nishihama, R., Ueda, M., Inoue, K., Ishida, S., Nishimura, Y., et al. (2015). Development of Gateway Binary Vector Series with Four Different Selection Markers for the Liverwort Marchantia polymorpha. *PLOS ONE* 10: e0138876.
Isken, O. and Maquat, L.E. (2007). Quality control of eukaryotic mRNA: safeguarding cells from abnormal mRNA function. *Genes Dev.* 21: 1833–1856.
Korner, C.G., Wormington, M., Muckenthaler, M., Schneider, S., Dehlin, E., and Wahle, E. (1998). The deadenylating nuclease (DAN) is involved in poly(A) tail removal during the meiotic maturation of Xenopus oocytes. *EMBO J.* 17: 5427–5437.
Kubota, A., Ishizaki, K., Hosaka, M., and Kohchi, T. (2013). Efficient Agrobacterium-Mediated Transformation of the Liverwort Marchantia polymorpha Using Regenerating Thalli. *Biosci. Biotechnol. Biochem.* 77: 167–172.
Lange, H., Sement, F.M., Canaday, J., and Gagliardi, D. (2009). Polyadenylation-assisted RNA degradation processes in plants. *Trends Plant Sci.* 14: 497–504.
Lupold, D.S., Caoile, A.G. and Stern, D.B. (1999). Polyadenylation occurs at multiple sites in maize mitochondrial *cox2* mRNA and is independent of editing status. *The Plant Cell* 11: 1565-1578.
Martin, G. and Keller, W. (2004). Sequence motifs that distinguish ATP(CTP):tRNA nucleotidyl transferases from eubacterial poly(A) polymerases. *RNA* 10: 899–906.
Mercer, T.R., Neph, S., Dinger, M.E., Crawford, J., Smith, M.A., Shearwood, A.-M.J., et al. (2011). The Human Mitochondrial Transcriptome. *Cell* 146: 645–658.
Minamino, N., Kanazawa, T., Era, A., Ebine, K., Nakano, A. and Ueda, T. (2018). RAB GTPases in the Basal Land Plant *Marchantia polymorpha*. *Plant Cell Physiol.* 59: 845-856.
Mohanty, B.K. and Kushner, S.R. (2010). Bacterial/archaeal/organellar polyadenylation. *Wiley Interdiscip. Rev. - RNA* 2: 256–276.
Montellese, C., Montel-Lehry, N., Henras, A.K., Kutay, U., Gleizes, P.-E., and O'Donohue, M.-F. (2017). Poly(A)-specific ribonuclease is a nuclear ribosome biogenesis factor involved in human 18S rRNA maturation. *Nucleic Acids Res.* 45: 6822–6836.
Moon, D.H., Segal, M., Boyraz, B., Guinan, E., Hofmann, I., Cahan, P., et al. (2015). Poly(A)-specific ribonuclease (PARN) mediates 3′-end maturation of the telomerase RNA component. *Nat. Genet.* 47: 1482–1488.
Nagaike, T., Suzuki, T., and Ueda, T. (2008). Polyadenylation in mammalian mitochondria: Insights from recent studies. *Biochim. Biophys. Acta BBA - Gene Regul. Mech.* 1779: 266–269.
Nagao, A., Hino-Shigi, N., and Suzuki, T. (2008). Measuring mRNA decay in human

mitochondria. *Methods Enzymol.* 447: 489–499.

Nilsson, P., Henriksson, N., Niedzwiecka, A., Balatsos, N.A., Kokkoris, K., Eriksson, J., et al. (2007). A multifunctional RNA recognition motif in poly(A)-specific ribonuclease with cap and poly(A) binding properties. *J. Biol. Chem.* 282: 32902–32911.

Nishimura, N., Kitahata, N., Seki, M., Narusaka, Y., Narusaka, M., Kuromori, T., et al. (2005). Analysis of ABA hypersensitive germination2 revealed the pivotal functions of PARN in stress response in Arabidopsis. *Plant J.* 44: 972–984.

Nishimura, N., Okamoto, M., Narusaka, M., Yasuda, M., Nakashita, H., Shinozaki, K., et al. (2009). ABA Hypersensitive Germination2-1 Causes the Activation of Both Abscisic Acid and Salicylic Acid Responses in Arabidopsis. *Plant Cell Physiol.* 50: 2112–2122.

Norbury, C.J. (2013). Cytoplasmic RNA: a case of the tail wagging the dog. *Nat. Rev. Mol. Cell Biol.* 14: 643–653.

Oda, K., Yamato, K., Ohta, E., Nakamura, Y., Takemura, M., Nozato, N., et al. (1992). Gene organization deduced from the complete sequence of liverwort Marchantia polymorpha mitochondrial DNA: A primitive form of plant mitochondrial genome. *J. Mol. Biol.* 223: 1–7.

Perrin, R., Meyer, E.H., Zaepfel, M., Kim, Y.J., Mache, R., Grienenberger, J.M., et al. (2004). Two exoribonucleases act sequentially to process mature 3'-ends of atp9 mRNAs in Arabidopsis mitochondria. *J. Biol. Chem.* 279: 25440-25446.

Reverdatto, S.V., Dutko, J.A., Chekanova, J.A., Hamilton, D.A., and Belostotsky, D.A. (2004). mRNA deadenylation by PARN is essential for embryogenesis in higher plants. *RNA* 10: 1200–1214.

Rorbach, J., Nicholls, T.J.J., and Minczuk, M. (2011). PDE12 removes mitochondrial RNA poly(A) tails and controls translation in human mitochondria. *Nucleic Acids Res.* 39: 7750–7763.

Salinas-Giegé, T., Cavaiuolo, M., Cognat, V., Ubrig, E., Remacle, C., Duchêne, A.-M., et al. (2017). Polycytidylation of mitochondrial mRNAs in Chlamydomonas reinhardtii. *Nucleic Acids Res.* 45: 12963–12973.

Shukla, S., Bjerke, G.A., Muhlrad, D., Yi, R., and Parker, R. (2019). The RNase PARN Controls the Levels of Specific miRNAs that Contribute to p53 Regulation. *Mol. Cell* 73: 1204-1216.e4.

Shukla, S., Schmidt, J.C., Goldfarb, K.C., Cech, T.R., and Parker, R. (2016). Inhibition of telomerase RNA decay rescues telomerase deficiency caused by dyskerin or PARN defects. *Nat. Struct. Mol. Biol.* 23: 286–292.

Stuart, B.D., Choi, J., Zaidi, S., Xing, C., Holohan, B., Chen, R., et al. (2015). Exome sequencing links mutations in PARN and RTEL1 with familial pulmonary fibrosis and

telomere shortening. *Nat. Genet.* 47: 512–517.

Sugano, S.S., Nishihama, R., Shirakawa, M., Takagi, J., Matsuda, Y., Ishida, S., et al. (2018). Efficient CRISPR/Cas9-based genome editing and its application to conditional genetic analysis in Marchantia polymorpha. *PLOS ONE* 13: e0205117.

Sugano, S.S., Shirakawa, M., Takagi, J., Matsuda, Y., Shimada, T., Hara-Nishimura, I., et al. (2014). CRISPR/Cas9-Mediated Targeted Mutagenesis in the Liverwort Marchantia polymorpha L. *Plant Cell Physiol.* 55: 475–481.

Tang, W., Tu, S., Lee, H.-C., Weng, Z., and Mello, C.C. (2016). The RNase PARN-1 Trims piRNA 3′ Ends to Promote Transcriptome Surveillance in C. elegans. *Cell* 164: 974–984.

Tomecki, R., Dmochowska, A., Gewartowski, K., Dziembowski, A., and Stepien, P.P. (2004). Identification of a novel human nuclear-encoded mitochondrial poly(A) polymerase. *Nucl Acids Res.* 32: 6001–6014.

Unseld, M., Marienfeld, J.R., Brandt, P., and Brennicke, A. (1997). The mitochondrial genome of Arabidopsis thaliana contains 57 genes in 366,924 nucleotides. *Nat. Genet.* 15: 57–61.

Weill, L., Belloc, E., Bava, F.-A., and Méndez, R. (2012). Translational control by changes in poly(A) tail length: recycling mRNAs. *Nat. Struct. Mol. Biol.* 19: 577–585.

Wilkie, G.S., Dickson, K.S., and Gray, N.K. (2003). Regulation of mRNA translation by 5′- and 3′-UTR-binding factors. *Trends Biochem. Sci.* 28: 182–188.

Wu, M., Nilsson, P., Henriksson, N., Niedzwiecka, A., Lim, M.K., Cheng, Z., et al. (2009). Structural Basis of m7GpppG Binding to Poly(A)-Specific Ribonuclease. *Structure* 17: 276–286.

Yoda, M., Cifuentes, D., Izumi, N., Sakaguchi, Y., Suzuki, T., Giraldez, A.J., et al. (2013). Poly(A)-Specific Ribonuclease Mediates 3′-End Trimming of Argonaute2-Cleaved Precursor MicroRNAs. *Cell Rep.* 5: 715–726.

Zimmer, S.L., Fei, Z., and Stern, D.B. (2008). Genome-based analysis of Chlamydomonas reinhardtii exoribonucleases and poly(A) polymerases predicts unexpected organellar and exosomal features. *Genetics* 179: 125–136.

Zimmer, S.L., Schein, A., Zipor, G., Stern, D.B., and Schuster, G. (2009). Polyadenylation in Arabidopsis and *Chlamydomonas* organelles: the input of nucleotidyltransferases, poly(A) polymerases and polynucleotide phosphorylase. *Plant J.* 59: 88–99.

Figure legends

Figure 1. Subcellular localization of Citrine fused MpAHG2 or MpAGS1 protein in *M. polymorpha* cell.

Transgenic *M. polymorpha* plants expressing constitutively MpAHG2-Citrine or MpAGS1-Citrine were constructed. Part of thallus of transgenic lines and wild type (WT, Tak-1) was excised and stained with MitoTracker and observed under laser-scanning microscope. The "magnified" panels show the enlarged images of the squared regions of the "merged" images.

Figure 2. Weak Mp*ahg2* mutants produced with the CRISPR/Cas9 genome editing methodology.

(A) Schematic representation of the Mp*AHG2* gene. Filled boxes and lines indicate exons and introns, respectively. Open triangles indicate the position of the target sites of CRISPR/Cas9 sgRNAs, filled triangle indicates the target sites described in panel (B). (B) Nucleotide sequences of the target (gRNA sequence in blue) and the edited sites. (C) Morphologies of the Mp*ahg2* mutants and wild type (WT, Tak-1) grown on the plate for 38 days. Scale bar indicates 20 mm. (D) Relative expression levels of Mp*AHG2*. The expression levels were normalized with Mp*EF1α* and expressed as relative levels to that of wild type (Tak-1). Error bars indicate SD (n = 3). * indicates significant difference between wild type ($p < 0.05$, Student's t-test).

Figure 3. Phenotype of the Mp*ags1* defective mutants.

(A) Schematic representation of the Mp*AGS1* genes. Black boxes and lines indicate exons and intron, respectively. The approximate positions of the targets of CRISPR/Cas9 sgRNAs are shown. (B) Nucleotide sequences around the target sites (gRNA sequence in blue) of wild type (Tak-1) and the obtained mutants, *Mpags1-1* (one bp insertion) and *Mpags1-2* (7 bp deletion). (C) Morphologies of the Mp*ags1* mutants and wild type (WT, Tak-1) grown on the plate for 40 days. Scale bar indicates 20 mm. (D) Fresh weight of the thallus of the Mp*ags1* mutants and wild type (Tak-1) grown on the plate for 30 days. Error bars indicate SD ($n \geq 13$). ** indicates significant difference between wild type ($p < 0.01$, Student's t-test).

Figure 4. Loss-of-function mutations of Mp*AHG2* in the Mp*ags1* mutant background.

(A) Nucleotide sequence around the target sites (gRNA sequence in blue) of wild type (Tak-1) and the obtained mutants, Mp*ahg2-4* and Mp*ahg2-5* (inserted nucleotides in red). (B) Morphologies of the thallus of wild type (WT, Tak-1), Mp*ags1-1*, and Mp*ags1*Mp*ahg2* double mutants grown on the plate for 35 days. Bar indicates 20 mm. (C) Fresh weight of the thallus grown on the plate for 30 days (mean ± SD, one-way ANOVA followed by Tukey's test ($p < 0.05$), $n \geq 10$).

Figure 5. *In vitro* deadenylase assay of MpAHG2.

(A) Structure of the RNA substrates. Gray bars indicate the sequence derived from a vector sequence. (B) Substrate RNAs were incubated with (+) or without (–) the recombinant MpAHG2 protein and analyzed by capillary electrophoresis. White triangles indicate substrate RNAs, black and gray triangles indicate major RNAs in the incubated samples. Asterisks indicate an RNase independent signal detected in all the protein samples obtained through the *in vitro* transcription-translation system.

Figure 6. Effect of Mp*AGS1* overexpression and Mp*ahg2* mutations on the poly(A) status of mitochondrial mRNA.

(A) Poly(A) tail-length assay for Mp*cox1* using RNA samples form wild type (Tak-1), Mp*AGS1* overexpression lines (#1, #6), and Mp*ahg2* mutants (Mp*ahg2-1*, Mp*ahg2-2*). Triangles indicate the DNA fragments specifically detected in the transgenic plants. (B) Nucleotide sequence of the indicated DNA fragment in (A).

Figure 7. Effect of Mp*AGS1* overexpression, Mp*ags1* mutation, and Mp*ahg2* mutation on the mitochondrial mRNA levels.

The transcript levels of Mp*cox1,* Mp*cob,* Mp*nad1,* Mp*nad5,* Mp*atp8* and *Mpatp9* were examined by qRT-PCR using the cDNA mixture synthesized with total RNA obtained wild type (Tak-1), Mp*AGS1* overexpressing lines (#1, #6), Mp*ags1*, and Mp*ahg2-1*. Transcript levels were normalized with a nuclear genome-coding gene for a mitochondrial ATP synthase subunit (*ATP synthase gamma*), and expressed as relative levels to that of wild type (Tak-1).

Error bars indicate the SD (n = 3). * and ** indicate the significant difference between wild type ($p < 0.05$ and 0.01, respectively, Student's t-test).

Figure 8. Complementation analysis of *Atahg2-1* by Mp*AHG2*.

(A) Morphologies of the wild-type (Col-0), *Atahg2-1*, and *Atahg2-1* expressing Mp*AHG2* (#1, #2) plants. Upper panels show the top views of three-week-old plants. Bottom panels show the side view of five-week-old plants. Bars indicate 20 mm. (B) Poly(A) tail-length assay for *Atcox1* and *Atnad7* using RNA samples from wild-type (Col), *Atahg2-1*, *Atahg2-1*+35S:Mp*AHG2* transgenic plants, and wild type+*35S*:Mp*AGS1* transgenic plants. Triangle indicates a PAT fragment. (C) The transcript levels of *Atcox1* and *Atnad7* were examined by qRT-PCR using the cDNA mixture synthesized with total RNA obtained from wild type (Col), *Atahg2-1*, *Atahg2-1+35S*:Mp*AHG2* transgenic plants, and wild type+*35S*:Mp*AGS1* transgenic plants. Transcript levels were normalized with *AtACT2* and expressed as relative levels to that of wild type (mean ± SD, one-way ANOVA followed by Tukey's test ($p < 0.05$), n = 3).

Supplemental data

Table S1. The results of circular RT-PCR assay for *AtORF107f* of *Atahg2-1* transgenic line expressing Mp*AHG2*.

Total of 33 cDNA clones were analyzed and nucleotide sequences of the 3' end, 5'end, additional nucleotide sequence, and the position of 3' end and 5'end were listed.

Table S2. List of oligonucleotides used in this study.

Figure S1. Rooted phylogenetic trees of MpAHG2 (A), MpAGS1 (B), and their related proteins in eukaryotes.

Scale bar indicates the average number of substitutions per site. The numbers in the phylogram nodes indicate percent bootstrap support from 1000 replicates for the phylogeny. Abbreviations indicate, At, *Arabidopsis thaliana*; AmTr, *Amborella trichopoda*; Smoe, *Selaginella moellendorffii*; Phpat, *Physcomitrella patens*; Mp, *Marchantia polymorpha*; kfl, *Klebsormidium nitens*; Ot, *Ostreococcus tauri*; Oluc, *Ostreococcus lucimarinus*; Bradi, *Brachypodium distachyon*; Nt, *Nicotiana tabacum*; Os, *Oryza sativa*; Potri, *Populus trichocarpa*; Hs, *Homo sapiens*; Xl, *Xenopus laevis*, respectively.

Figure S2. Alignments of amino acid sequences of MpAGS1, MpAHG2 and their homologs in plants.

(A) Alignment of MpAHG2 and its homologs. Blue and red boxes indicate R3H and RRM motifs conserved among animal PARNs, which are required for CAP binding activity of these PARNs. (B) Alignment of MpAGS1 and its homologs. Black box indicates the conserved motifs found specifically in PAP but not in CCA transferase. Abbreviations indicate, At, *Arabidopsis thaliana*; AmTr, *Amborella trichopoda*; Phpat, *Physcomitrella patens*; Mp, *Marchantia polymorpha*; kfl, *Klebsormidium nitens*; Bradi, *Brachypodium distachyon*; Os, *Oryza sativa*; Hs, *Homo sapiens*; Xl, *Xenopus laevis*, respectively.

Figure S3. Growth of the Mp*ahg2-1,* Mp*ahg2-2* and Mp*ahg2-3.*

The area of thallus of Mp*ahg2-1,* Mp*ahg2-2,* and Mp*agh2-3* grown on the agar plates on 20 to 30 days were measured using Image J and shown as a relative value against that of wild type (Tak-1) on the same plate (mean ± SD, n = 4).

Figure S4. Mutation of the Mp*ahg2-6* mutant.

(A) Nucleotide sequences around the target2 used in the CRISPR/Cas9 experiments of the wild type (Tak-1) and Mp*ags1-2*Mp*ahg2-6*. (B) Morphologies of wild type (WT, Tak-1) and the mutant lines grown on the plate for 30 days. Scale bar indicates 30 mm.

Figure S5. Detection of recombinant MpAGS1 and MpAHG2 proteins.

Purified proteins obtained with a wheat germ protein expression system were separated on the SDS-PAGE gel, then transferred to a PVDF membrane. The recombinant proteins were detected with anti-MYC-epitope tag antibody.

Figure S6. The Mp*AGS1*-overexpression lines.

(A) Morphologies of wild type and the MpAGS1 overexpression lines (#1, #6) grown on the plate for 38 days. (B) The relative transcript levels of Mp*AGS1* (upper panels) or Mp*AHG2* (lower panel) in the Mp*AGS1*-overexpression lines, Mp*ags1-2*, and Mp*ahg2-1*. The transcript levels were examined by qRT-PCR using the cDNA mixture synthesized with total RNA obtained from these lines (the same RNA samples used in the experiments shown in Figure 8). Transcript levels were normalized with the Mp*EF1α* gene and expressed as relative levels to that of wild type (Tak-1). Error bars indicate the SD (n = 4). * and ** indicate the significant difference between wild type ($p < 0.05$ and 0.01, respectively, Student's t-test).

Figure S7. Rosette leaf areas of Arabidopsis lines.

(A) The rosette leaf areas of three-week-old wild-type (Col-0), *Atahg2-1*, *Atahg2-1* expressing Mp*AHG2* (#1, #2) plants were measured using Image J (mean ± SD, one-way ANOVA followed by Tukey's test ($p < 0.05$), n = 4). (B) Morphologies of the 4-week-old Mp*AGS1* expressing transgenic Arabidopsis lines.

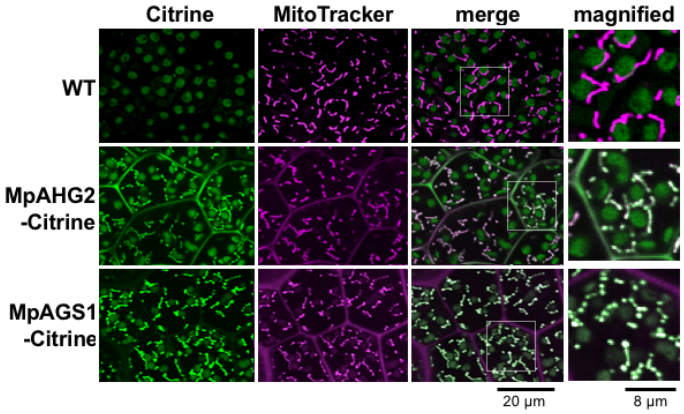

Figure 1. Subcellular localization of Citrine fused MpAHG2 or MpAGS1 protein in *M. polymorpha* cell. Transgenic *M. polymorpha* plants expressing constitutively MpAHG2-Citrine or MpAGS1-Citrine were constructed. Part of thallus of transgenic lines and wild type (WT, Tak-1) was excised and stained with MitoTracker and observed under laser-scanning microscope. The "magnified" panels show the enlarged images of the squared regions of the "merged" images.

190x275mm (96 x 96 DPI)

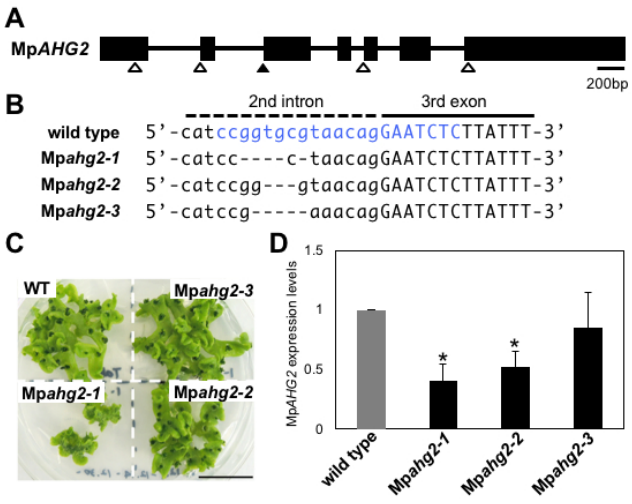

Figure 2. Weak Mp*ahg2* mutants produced with the CRISPR/Cas9 genome editing methodology. (A) Schematic representation of the Mp*AHG2* gene. Filled boxes and lines indicate exons and introns, respectively. Open triangles indicate the position of the target sites of CRISPR/Cas9 sgRNAs, filled triangle indicates the target sites described in panel (B). (B) Nucleotide sequences of the target (gRNA sequence in blue) and the edited sites. (C) Morphologies of the Mp*ahg2* mutants and wild type (WT, Tak-1) grown on the plate for 38 days. Scale bar indicates 20 mm. (D) Relative expression levels of Mp*AHG2*. The expression levels were normalized with Mp*EF1α* and expressed as relative levels to that of wild type (Tak-1). Error bars indicate SD (n = 3). * indicates significant difference between wild type ($p < 0.05$, Student's t-test).

190x275mm (96 x 96 DPI)

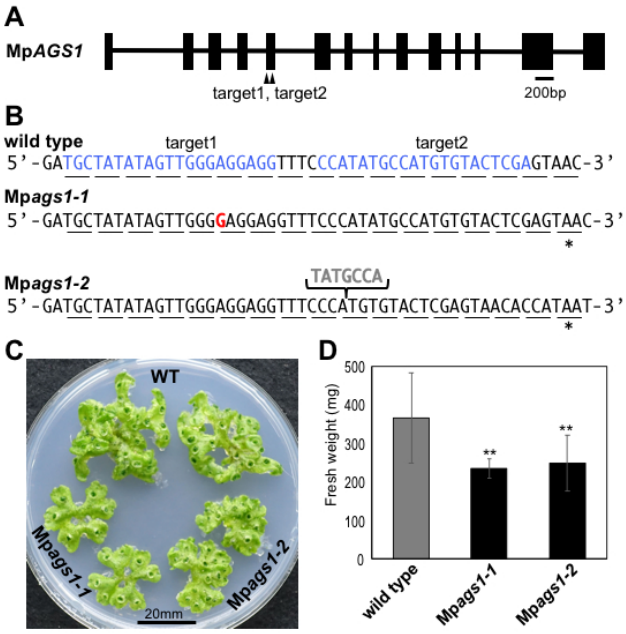

Figure 3. Phenotype of the Mp*ags1* defective mutants.
(A) Schematic representation of the Mp*AGS1* genes. Black boxes and lines indicate exons and intron, respectively. The approximate positions of the targets of CRISPR/Cas9 sgRNAs are shown. (B) Nucleotide sequences around the target sites (gRNA sequence in blue) of wild type (Tak-1) and the obtained mutants, Mp*ags1-1* (one bp insertion) and Mp*ags1-2* (7 bp deletion). (C) Morphologies of the Mp*ags1* mutants and wild type (WT, Tak-1) grown on the plate for 40 days. Scale bar indicates 20 mm. (D) Fresh weight of the thallus of the Mp*ags1* mutants and wild type (Tak-1) grown on the plate for 30 days. Error bars indicate SD ($n \geq 13$). ** indicates significant difference between wild type ($p < 0.01$, Student's t-test).

190x275mm (96 x 96 DPI)

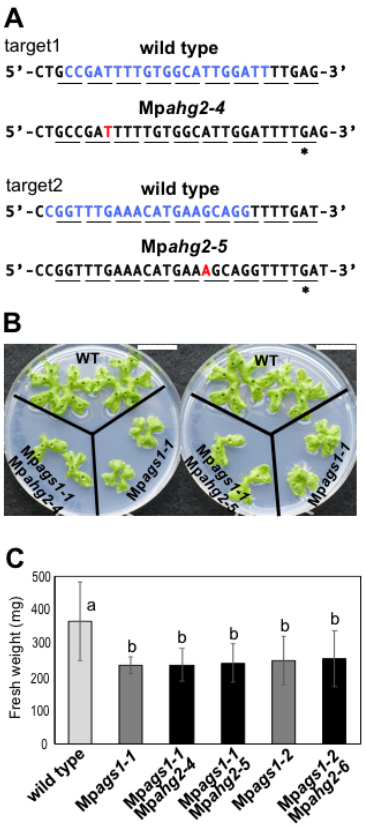

Figure 4. Loss-of-function mutations of Mp*AHG2* in the Mp*ags1* mutant background.
(A) Nucleotide sequence around the target sites (gRNA sequence in blue) of wild type (Tak-1) and the obtained mutants, Mp*ahg2-4* and Mp*ahg2-5* (inserted nucleotides in red). (B) Morphologies of the thallus of wild type (WT, Tak-1), Mp*ags1-1*, and Mp*ags1*Mp*ahg2* double mutants grown on the plate for 35 days. Bar indicates 20 mm. (C) Fresh weight of the thallus grown on the plate for 30 days (mean ± SD, one-way ANOVA followed by Tukey's test ($p < 0.05$), $n \geq 10$).

190x275mm (96 x 96 DPI)

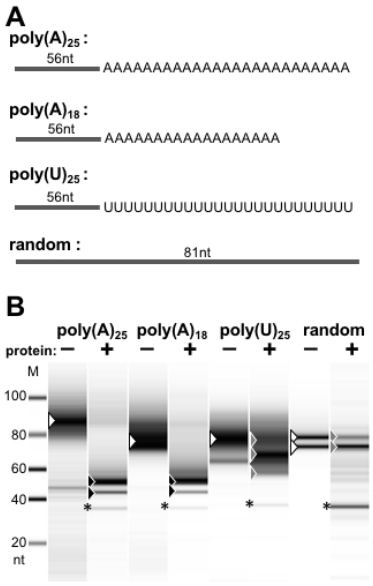

Figure 5. In vitro deadenylase assay of MpAHG2.
(A) Structure of the RNA substrates. Gray bars indicate the sequence derived from a vector sequence. (B) Substrate RNAs were incubated with (+) or without (−) the recombinant MpAHG2 protein and analyzed by capillary electrophoresis. White triangles indicate substrate RNAs, black and gray triangles indicate major RNAs in the incubated samples. Asterisks indicate an RNase independent signal detected in all the protein samples obtained through the *in vitro* transcription-translation system.

190x275mm (96 x 96 DPI)

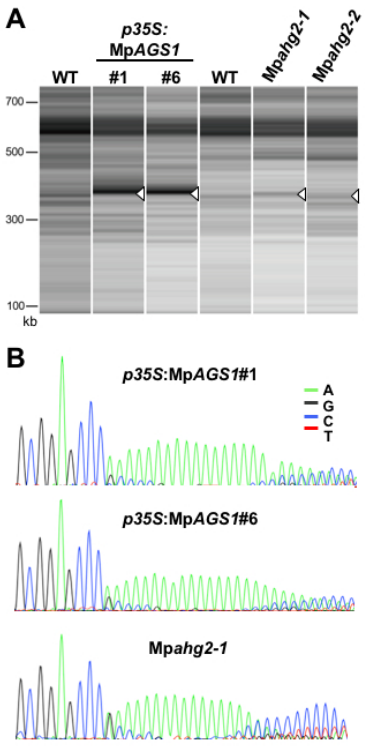

Figure 6. Effect of Mp*AGS1* overexpression and Mp*ahg2* mutations on the poly(A) status of mitochondrial mRNA.
(A) Poly(A) tail-length assay for Mp*cox1* using RNA samples form wild type (Tak-1), Mp*AGS1* overexpression lines (#1, #6), and Mp*ahg2* mutants (Mp*ahg2-1*, Mp*ahg2-2*). Triangles indicate the DNA fragments specifically detected in the transgenic plants. (B) Nucleotide sequence of the indicated DNA fragment in (A).

190x275mm (96 x 96 DPI)

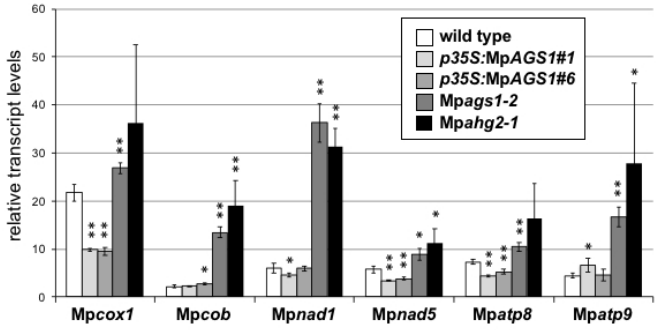

Figure 7. Effect of Mp*AGS1* overexpression, Mp*ags1* mutation, and Mp*ahg2* mutation on the mitochondrial mRNA levels. "The transcript levels of Mp*cox1*, Mp*cob*, Mp*nad1*, Mp*nad5*, Mp*atp8* and Mp*atp9* were examined by qRT-PCR using the cDNA mixture synthesized with total RNA obtained wild type (Tak-1), Mp*AGS1* overexpressing lines (#1, #6), Mp*ags1*, and Mp*ahg2-1*. Transcript levels were normalized with a nuclear genome-coding gene for a mitochondrial ATP synthase subunit (ATP synthase gamma), and expressed as relative levels to that of wild type (Tak-1). Error bars indicate the SD (n = 3). * and ** indicate the significant difference between wild type ($p < 0.05$ and 0.01, respectively, Student's t-test).

190x275mm (96 x 96 DPI)

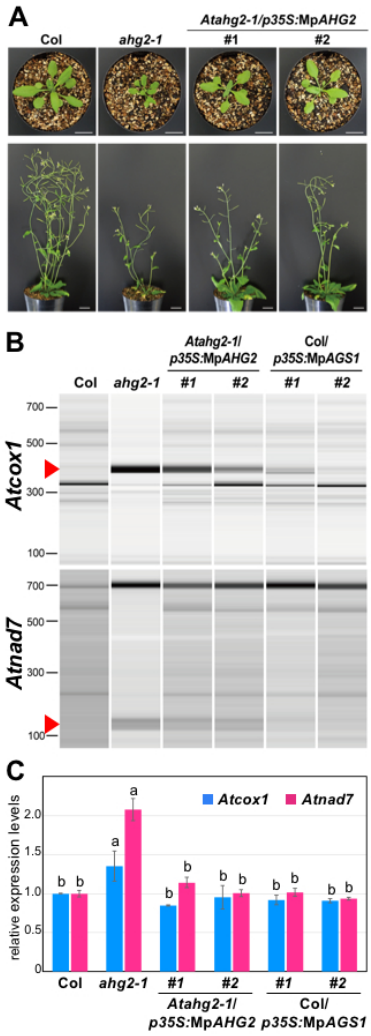

Figure 8. Complementation analysis of *Atahg2-1* by Mp*AHG2*. (A) Morphologies of the wild-type (Col-0), *Atahg2-1*, and *Atahg2-1* expressing Mp*AHG2* (#1, #2) plants. Upper panels show the top views of three-week-old plants. Bottom panels show the side view of five-week-old plants. Bars indicate 20 mm. (B) Poly(A) tail-length assay for *Atcox1* and *Atnad7* using RNA samples from wild-type (Col), *Atahg2-1*, *Atahg2-1+35S*:Mp*AHG2* transgenic plants, and wild type+*35S*:Mp*AGS1* transgenic plants. Triangle indicates a PAT fragment. (C) The transcript levels of *Atcox1* and *Atnad7* were examined by qRT-PCR using the cDNA mixture synthesized with total RNA obtained from wild type (Col), *Atahg2-1*, *Atahg2-1+35S*:Mp*AHG2* transgenic plants, and wild type+*35S*:Mp*AGS1* transgenic plants. Transcript levels were normalized with *AtACT2* and expressed as relative levels to that of wild type (mean ± SD, one-way ANOVA followed by Tukey's test ($p < 0.05$), n = 3).

190x275mm (96 x 96 DPI)

Table S1. cRT-PCR assay of orf107 in Atahg2-1/MpAHG2#1 line

Sequence of 3' end	addtional sequence	sequence of 5'end	position of 3' end	position of 5' end
AAAGGGAGGGAAGG	ttg	GATATGGTTTGACCC	270409	270647
AAAGGGAGGGAAGGCTAGGTCTT	AAAAAAAA	ATGGTTTGACCC	270400	270644
AAAGGGAGGGAAGGCTAGGTCTT	AAAAAAAA	ATGGTTTGACCC	270400	270644
AAAGGGAGGGAAGGCTAGGTCTT	AAAAAAAA	ATGGTTTGACCC	270400	270644
AAAGGGAGGGAAGGCTAGGTCTTT	AAAAAAAA	ATGGTTTGACCC	270399	270644
AAAGGGAGGGAAGG	AAAA	ATGGTTTGACCC	270409	270644
AAAGGGAGGGAAGGC	AA	AAGATATGGTTTGACCC	270408	270649
AAAGGGAGGGAAGGCTA	AA	ATGGTTTGACCC	270406	270644
AAAGGGAGGGAAGGCTAGGTCTTT	A	ATATGGTTTGACCC	270399	270646
ACAAAAAAGGC		ATGGTTTGACCC	270494	270644
CAAAAAAGGCCATGAATG		ATGGTTTGACCC	270486	270644
AAAGGGAGGGAAGG		GTAAGATATGGTTTGACCC	270409	270651
AAAGGGAGGGAAGG		TGGTTTGACCC	270409	270643
AAAGGGAGGGAAGGC		ATGGTTTGACCC	270408	270644
AAAGGGAGGGAAGGC		ATGGTTTGACCC	270408	270644
AAAGGGAGGGAAGGC		ATGGTTTGACCC	270408	270644
AAAGGGAGGGAAGGCT		GATATGGTTTGACCC	270407	270647
AAAGGGAGGGAAGGCT		GATATGGTTTGACCC	270407	270647
AAAGGGAGGGAAGGCT		GATATGGTTTGACCC	270407	270647
AAAGGGAGGGAAGGCT		GATATGGTTTGACCC	270407	270647
AAAGGGAGGGAAGGCT		GGTTTGACCC	270407	270642
AAAGGGAGGGAAGGCTAGGTCT		ATGGTTTGACCC	270401	270644
AAAGGGAGGGAAGGCTAGGTCT		ATGGTTTGACCC	270401	270644
AAAGGGAGGGAAGGCTAGGTCT		ATGGTTTGACCC	270401	270644
AAAGGGAGGGAAGGCTAGGTCTT		ATGGTTTGACCC	270400	270644
AAAGGGAGGGAAGGCTAGGTCTT		ATGGTTTGACCC	270400	270644
AAAGGGAGGGAAGGCTAGGTCTTT		TGGTTTGACCC	270399	270643
AAAGGGAGGGAAGGCTAGGTCTTT		TGGTTTGACCC	270399	270643
AAAGGGAGGGAAGGCTAGGTCTTTCC		GATATGGTTTGACCC	270397	270647
AAAGGGAGGGAAGGCTAGGTCTTTCC		GATATGGTTTGACCC	270397	270647
AAAGGGAGGGAAGGCTAGGTCTTTCC		GATATGGTTTGACCC	270397	270647
AAAGGGAGGGAAGGCTAGGTCTTTCC		GATATGGTTTGACCC	270397	270647
AAAGGGAGGGAAGGCTAGGTCTTTCC		GATATGGTTTGACCC	270397	270647

Table S2. Primers used in this study

Name	Sequence	Usage
MpAHG2attB1	AAAAAGCAGGCTccATGGCGCCTAGTCGCCTGCTG	cDNA cloning
MpAHG2stopC	AGAAAGCTGGGTATTACACGTCTTTCGGATCTTC	cDNA cloning without Stop codon
MpAHG2attB2	AGAAAGCTGGGTaCACGTCTTTCGGATCTTCAAGG	cDNA cloning
MpAGS1attB1	AAAAAGCAGGCTccATGACAACATCGGTGGCTCTG	cDNA cloning
MpAGS1stopC	AGAAAGCTGGGTATTATGTCTTAACTTCTCGAGG	cDNA cloning without stop codon
MpAGS1attB2	AGAAAGCTGGGTaTGTCTTAACTTCTCGAGGATAC	cDNA cloning
MpAHG2-mitF3	TTACCTCTCACTA AATCTCCTCCGAAGACG	cDNA cloning without singal sequence
MpAGS1-mitF3	TTACCTCTCACTA ATGTGGCTCGCACTCC	cDNA cloning without singal sequence
Mtsig-B1	AAAAAGCAGGCTTGATGTCATCGATTGTGAATCGAGC	Arabidopsis Mit signal sequence
MITSIGR2	AGTGAGAGGTAAGAAGTCCCG	Arabidopsis Mit signal sequence
attB1	GGGGACAAGTTTGTACaaAAAAGCAGGCT	BP reaction sequence
attB2	GGGGACCACTTTGTAcaAGAAAGCTGGGT	BP reaction sequence
MpAHG2F1	AGGTTCTAGTGGACGC	sequencing
MpAHG2R1	TCCTGATGAGAACTTG	sequencing
MpAHG2F2	ACGGAACGAGCTTCCTGTAG	sequencing
MpAGS1F1	GCAGTGTTCGTGATCT	sequencing
pDONR1	CGCGTTAACGCTAGCA	sequencing
pDONR2	GTAACATCAGAGATTT	sequencing
MpAHG2_CC_F1n	TCTCGAATCCAATGCCACAAAAT	guideRNA
MpAHG2_CC_R1n	AAACATTTTGTGGCATTGGATTC	guideRNA
MpAHG2_CC_F2n	TCTCGCGGTTTGAAACATGAAGC	guideRNA
MpAHG2_CC_R2n	AAACGCTTCATGTTTCAAACCGC	guideRNA
MpAHG2_CC_F3n	TCTCGAAATTATATCTGTACAAG	guideRNA
MpAHG2_CC_R3n	AAACCTTGTACAGATATAATTTC	guideRNA
MpAHG2_CC_F4n	TCTCGAGATTCCTGTTACGCAC	guideRNA
MpAHG2_CC_R4n	AAACGTGCGTAACAGGAATCTC	guideRNA
MpAHG2_CC_F5n	TCTCGTCTAACTCCTTCTGTAAA	guideRNA
MpAHG2_CC_R5n	AAACTTTACAGAAGGAGTTAGAC	guideRNA
proMpU6-1-F1	GGCCTCATTTATTGCACCATAC	sequencing
MpAHG2_CC_F1	CATTAGCATGCGGAGAATTC	sequencing
MpAHG2_CC_R1	GGTGTTACTGAAGGCAAATATTC	sequencing
MpAHG2_CC_F2	GCGAATAGTAGGAGTACGTC	sequencing
MpAHG2_CC_R2	GCATGAAGGCCTCCAATAT	sequencing
MpAHG2_CC_F3	AACAGGAGAAGGTTTCGTGC	sequencing
MpAHG2_CC_R3	TACCACAACGTCCTGCGTCC	sequencing
MpAHG2_CC_F4	AGTGGAATTGGTGAGTGCCG	sequencing
MpAHG2_CC_R4	CTCTCACTTGCTTGACCAGC	sequencing
MpAHG2_CC_F5	ACAGCAGGCAACTCATGTCC	sequencing
MpAHG2_CC_R5	TGAAGAGTTGGGCACTGACC	sequencing
T7dTprimer	GGCCAGTGAATTGTAATACGACTCACTATAGGGAGGCGGTTTTTTTTTTTTTT	cDNA synthesis for PAT assay
T7 proUni	TAATACGACTCACTATAGGG	PAT assay
MpCOX1F1	CGCTTGCAGGTATGCCACGTCG	PAT assay, qRTPCR
MpCOX1R1	CGGAGGGCTTGGGACCATCC	qRTPCR
MpATP9F	TGATGGATTTCGCGCAACAG	qRTPCR
MpATP9R	AGGTGCAAAATTAATTGGAGCAGG	qRTPCR
MpNAD5F	GACGTCATTCTTCGCGGCAACC	qRTPCR
MpNAD5R	CAGAATAGTTGGAAATGCCGCAAGC	qRTPCR
MpNAD1F	TAGATAACCGAATCCGGAGTAGCC	qRTPCR
MpNAD1R	GTTAACTCATGCGCTCTAACCCTAGC	qRTPCR
MpCOBF	CTTCGAGAGAAGAGGAGACGGC	qRTPCR
MpCOBR	GGAGACTCGTTCCATGACTTCGC	qRTPCR
MpATP8F	CAGAGCAATGACCGTGTAGAACAGG	qRTPCR
MpATP8R	TGAGCATTTGCGAGTTGGACCATTCC	qRTPCR
MpAHG2F2	GTGAAAGTTGAGATTGCTAGCGAAC	qRTPCR
MpAHG2R2	GACCGTATTG TAGCAGTGTC	qRTPCR
MpAGS1F2	AGCTTACAGGGGCTGAACCTG	qRTPCR
MpAGS1R2	GCTTCCTGCCGATGCTTGG	qRTPCR
MpASgF1	ATTGACAGCTGCCAGTGGTCCGG	qRTPCR
MpASgR1	ATCTGTGAGCGTGGATGCCAGGGA	qRTPCR
MpEF1F	AAGCCGTCGAAAAGAAGGAG	qRTPCR
MpEF1R	TTCAGGATCGTCCGTTATCC	qRTPCR
Mp_male-F1	CCAAGTGCGGGCAGAATCAAGT	sex determination
Mp_male-R1	TTCATCGCCCGCTATCACCTTC	sex determination
Mp_female-F1	GACGACGAAGATGTGGATGAC	sex determination
Mp_female-R1	GAAACTTGGCCGTGTGACTGA	sex determination
Atnad7pat	TGTGTTTGGAGAGGTGGATAGATAG	PAT assay
Atcox1pat	TAGGGCTTTCAGGTATGCCACGTCG	PAT assay
Atcox1F1	GTCTTCGGGTATCTAGGCATGG	qRTPCR
Atcox1R1	CCAGTGAGTCCTCCTATGGTG	qRTPCR
Atnad7F1	GATTCGCGAAGAGCAGCACC	qRTPCR
Atnad7R1	GGACATAGCTTACGATCATCGGC	qRTPCR
pGEM4zrand	TAGGTGACACTATAGAATACGAAT	RNA substrate synthesis
pGEM4zpolyAS	TTTTTTTTTTTTTTTTTTCGAGCTCGGTACCCG	RNA substrate synthesis
pGEM4zpolyA	TTTTTTTTTTTTTTTTTTTTTTTTTTCGAGCTCGGTACCCG	RNA substrate synthesis
pGEM4zpolyU	AAAAAAAAAAAAAAAAAAAAAAAAACGAGCTCGGTACCCG	RNA substrate synthesis
ORF107fcRTF	GGAACGCCTCAGGTCGAATGAATACG	circular RT-PCR
ORF107fcRTR1	CGTATTCATTCGACCTGAGGCG	circular RT-PCR
ORF107fcRTR2	CATGCTCTGGTTCCGGG	circular RT-PCR

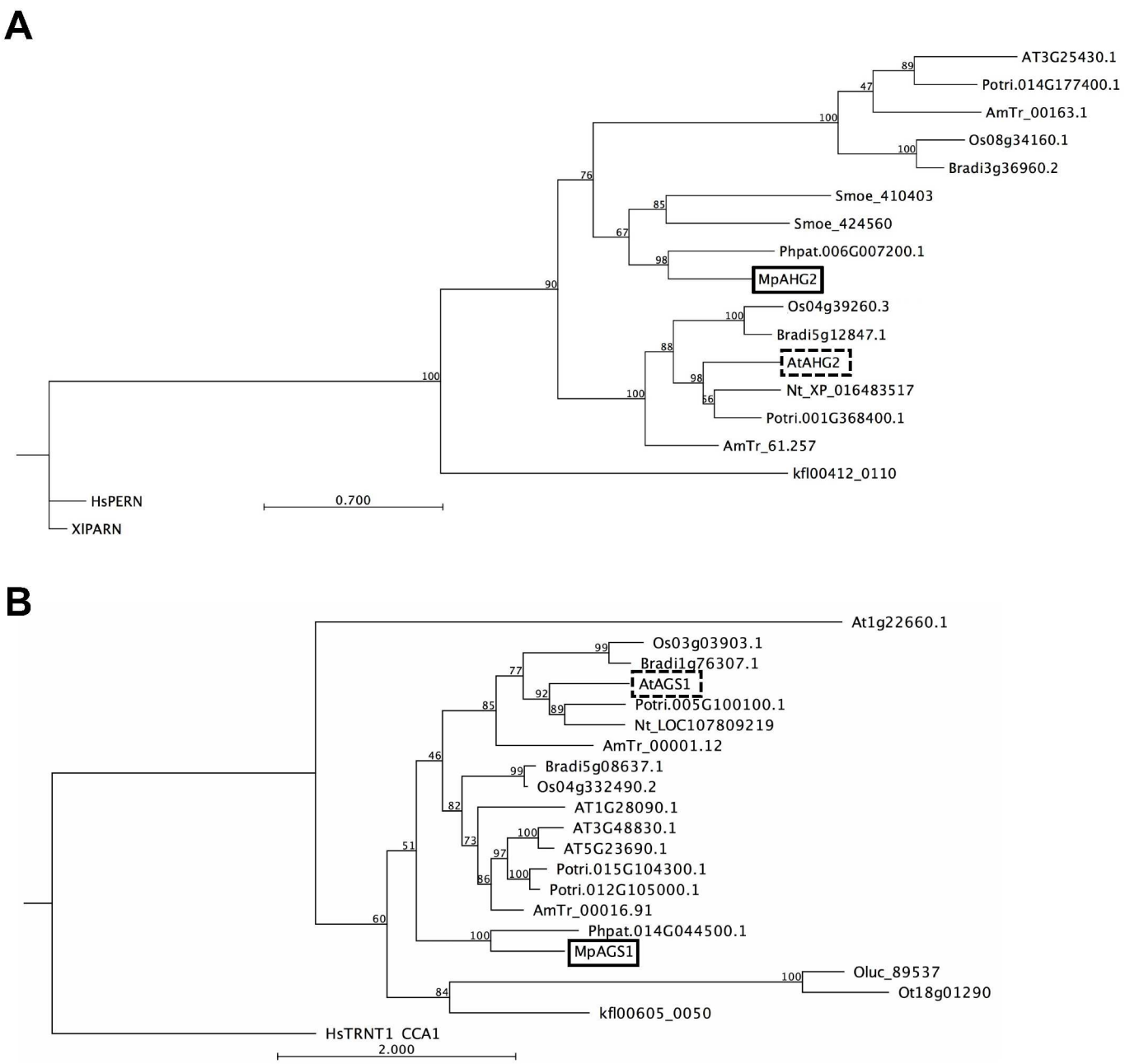
A
AT3G25430.1
Potri.014G177400.1
AmTr_00163.1
Os08g34160.1
Bradi3g36960.2
Smoe_410403
Smoe_424560
Phpat.006G007200.1
MpAHG2
Os04g39260.3
Bradi5g12847.1
AtAHG2
Nt_XP_016483517
Potri.001G368400.1
AmTr_61.257
kfl00412_0110
HsPERN
XIPARN
0.700
B
At1g22660.1
Os03g03903.1
Bradi1g76307.1
AtAGS1
Potri.005G100100.1
Nt_LOC107809219
AmTr_00001.12
Bradi5g08637.1
Os04g332490.2
AT1G28090.1
AT3G48830.1
AT5G23690.1
Potri.015G104300.1
Potri.012G105000.1
AmTr_00016.91
Phpat.014G044500.1
MpAGS1
Oluc_89537
Ot18g01290
kfl00605_0050
HsTRNT1_CCA1
2.000

Fig. S2A

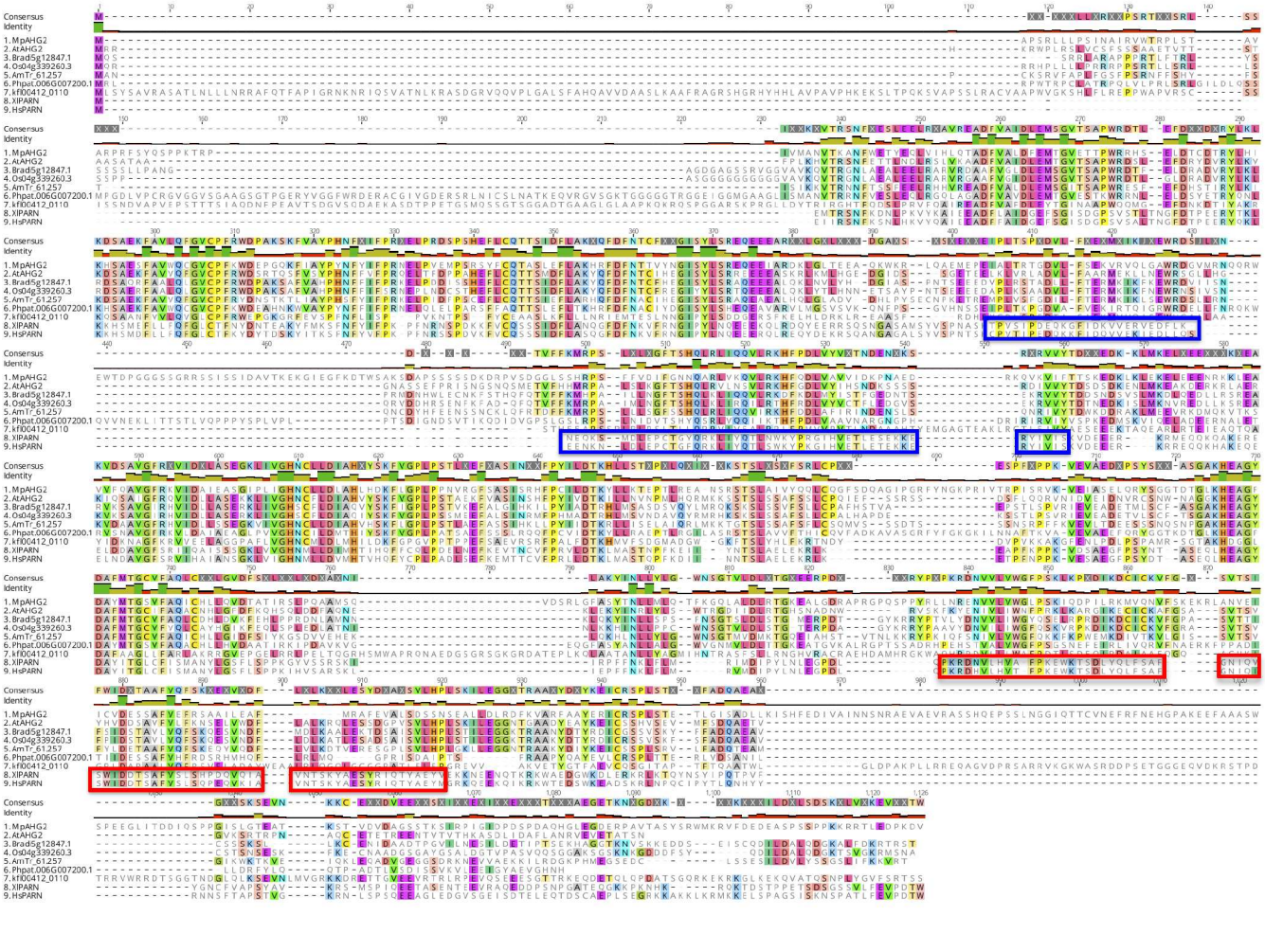


Consensus
Identity
1. MpAGS1
2. AtAGS1
3. Bradi1g76307.1
4. Os03g03930.1
5. AmTr_00001.12
6. Phpat.014G044500.1
7. kfl00605_0050

Fig. S3

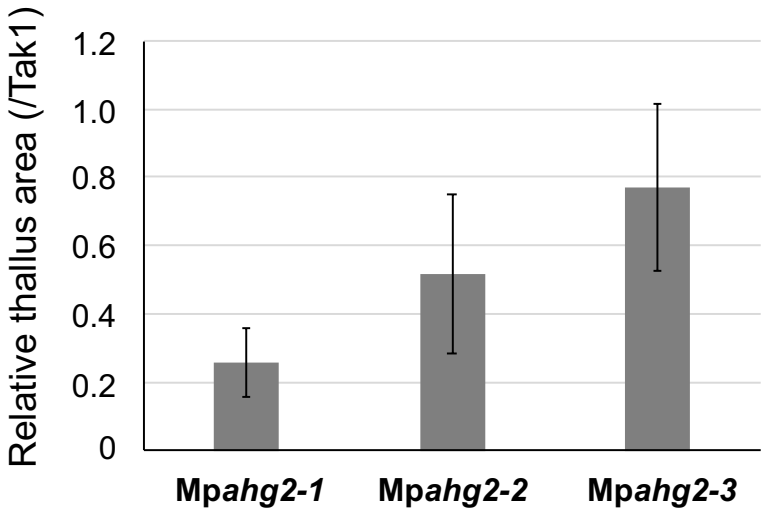
Relative thallus area (/Tak1)
1.2
1.0
0.8
0.6
0.4
0.2
0
Mpahg2-1
Mpahg2-2
Mpahg2-3

A

target2

wild type: 5’-…CCGGTTTGAAACATGAAGCAGGTTTTGAT…-3’

Mp*ahg2-6*:

CAAACCAAATGTCCTGGGACCATTACCACCAAACGTTTCAAA

B

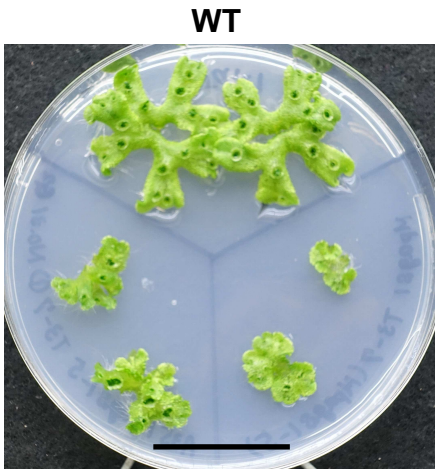

Fig. S5

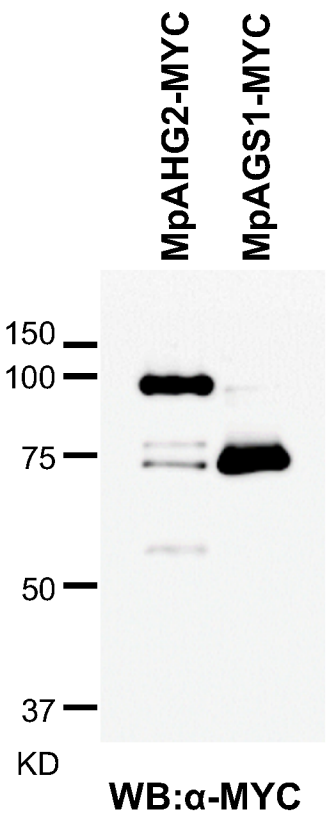

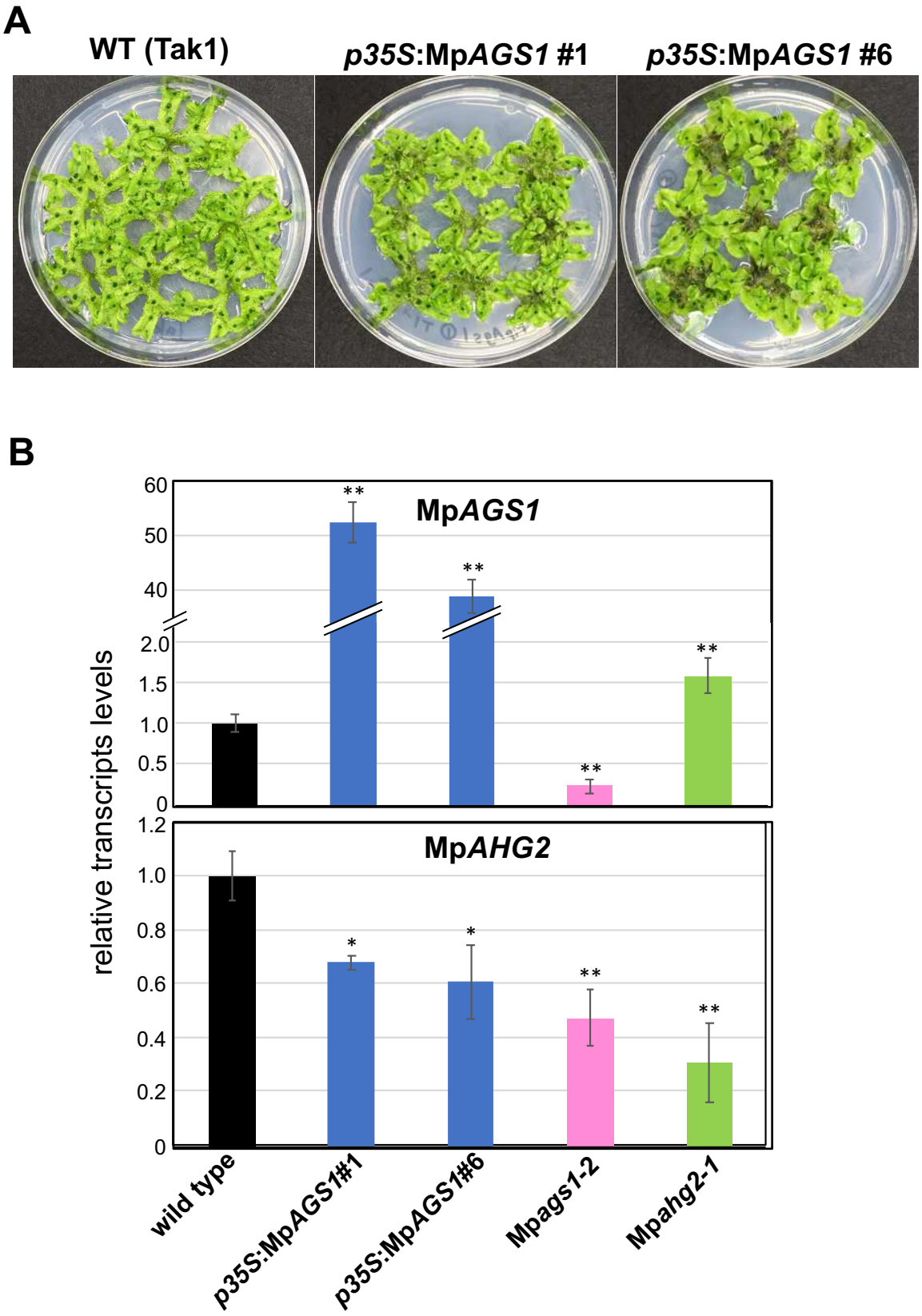
A
WT (Tak1)
p35S:MpAGS1 #1
p35S:MpAGS1 #6
B
MpAGS1
MpAHG2
relative transcripts levels
60
50
40
2.0
1.5
1.0
0.5
0
1.2
1.0
0.8
0.6
0.4
0.2
0
**
*
wild type
p35S:MpAGS1#1
p35S:MpAGS1#6
Mpags1-2
Mpahg2-1

Fig. S7

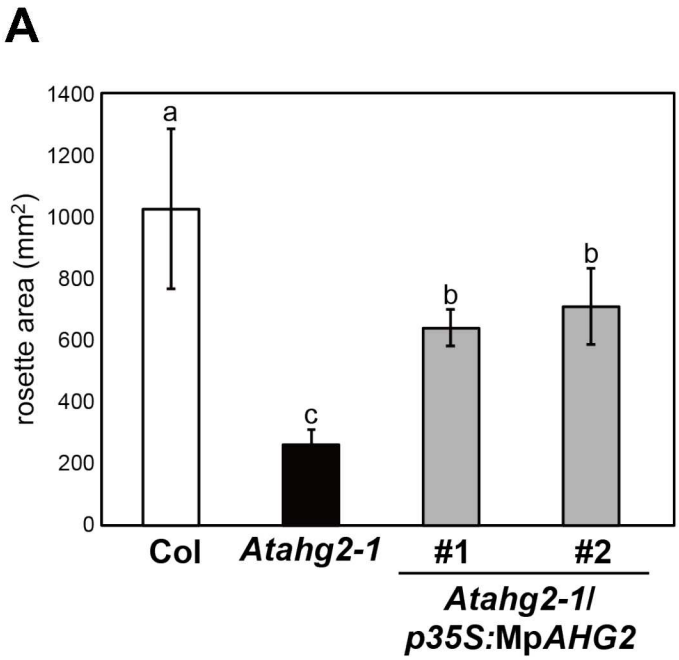
A
1400
1200
1000
800
600
400
200
0
rosette area (mm2)
a
c
b
b
Col
Atahg2-1
#1
#2
Atahg2-1/
p35S:MpAHG2

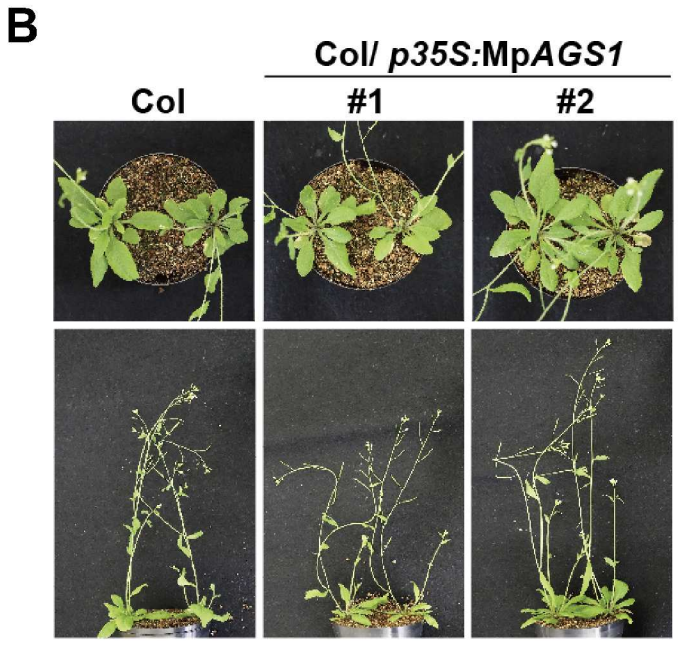
B
Col/ p35S:MpAGS1
Col
#1
#2